Spin-density waves and itinerant antiferromagnetism in metals

N. I. Kulikov and V. V. Tugushev

Institute of High-Pressure Physics, Moscow Province
Usp. Fiz. Nauk **144**, 643–680 (December 1984)

The present state of the theory and the main experimental results are reviewed for systems in which the antiferromagnetic ordering is directly due to a peculiar topology of the Fermi surface, i.e., to the presence of nested electron and hole sheets. A familiar example of such a system is chromium, which supports a spin-density wave (SDW) that is incommensurate with the lattice. For this reason much of the experimental material discussed in this review is for chromium and its alloys with transition and nontransition metals. The theoretical description of SDWs of this type is based on the excitonic insulator model, which is discussed in detail not only in connection with the phase diagrams and SDW structure but also in regard to the electronic properties of systems of this type (measurements of the de Haas–van Alphen effect, optical measurements, band-structure calculations from first principles, etc.). The review concludes with a discussion of less-studied transition-metal compounds which apparently also support a SDW state due to a peculiar topology of the Fermi surface.

CONTENTS

1. INTRODUCTION

The concept of spin-density waves (SDWs) and charge-density waves (CDWs) has become very popular in recent years in the study of electronic, magnetic, and structural phase transitions. Here we attempt to elucidate the most interesting experimental and theoretical results of the past decade which have contributed to our understanding of the properties of itinerant antiferromagnets which undergo a transition to a SDW state. Specifically, we discuss three-dimensional metals whose Fermi surfaces have nearly nested (coincident upon translation by some wave vector $\tilde{\mathbf{Q}}$) electron and hole portions. Such a topology of the Fermi surface makes it possible to have triple electron-hole pairing with the onset of an antiferromagnetic structure with wave vector $\mathbf{Q}$ close to $\tilde{\mathbf{Q}}$.

It is well known that the theory of itinerant magnetism contains an approximate criterion for instability of the paramagnetic ground state with respect to some sort of magnetic ordering (the generalized Hubbard-Stoner criterion). In particular, for the simplest antiferromagnetic-transition model with an effective electron-electron interaction potential I this criterion is

$$1 = I\chi(\mathbf{Q}), \tag{1}$$

where $\chi(\mathbf{Q})$ is the magnetic susceptibility of noninteracting quasiparticles in the Hartree-Fock approximation and $\mathbf{Q}$ is the characteristic wave vector of the antiferromagnetic structure. Whether this criterion is satisfied or not depends not only on the value of I itself but also on the dependence of the susceptibility $\chi(\mathbf{q})$ on the wave vector $\mathbf{q}$. If, because of some topological feature of the Fermi surface, $\chi(\mathbf{q})$ has a pronounced maximum at $\mathbf{q} = \mathbf{Q}$, the instability criterion can be satisfied even at small values of I ($I \ll N(0)^{-1}$, where $N(0)$ is the density of electronic states of the nested portions at the Fermi energy). The presence of a small interaction parameter $IN(0) \ll 1$ enables one to construct a successful theoretical model having an asymptotically exact solution in the mean field approximation (the "excitonic insulator" model). This model, as can be seen from a comparison with experiment, works rather well for describing an important class of real metallic antiferromagnets.

The self-consistent theory of spin fluctuations that was proposed by Moriya and coworkers (reviewed in Ref. 51) ignores the topological features of the Fermi surface of itinerant antiferromagnets and postulates a choice of wave vector $\mathbf{Q}$ of the antiferromagnetic structure in accordance with a particular experimental situation. Here the antiferromagnetism criterion should be satisfied for comparatively large values of the interaction potential I ($IN(0) \approx 1$), i.e., outside the applicability region of mean field theory. The lack of a small interaction parameter makes it difficult to control the approximations in the self-consistent theory of spin fluctuations.

In the case of a rather large interaction potential

 0038-5670/84/120954-23$01.80

($IN(0) > 1$) the magnetic moments cannot be handled by the orthodox treatments of itinerant magnetism (i.e., as completely delocalized) and one must take an approach which combines features of the itinerant and Heisenberg models of magnetic ordering. Many authors have constructed versions of interpolation theories based on some technique of evaluating the local spin fluctuations (a history of this problem is given by Moriya[9]). The method proposed by Moriya and Usami[51] has yielded a connection between the local and self-consistent spin-fluctuation theories: the first theory reduces to the second for $IN(0) - 1 \ll 1$.

For antiferromagnets the theory of local spin fluctuations was developed by Hasegawa[52] (see also Grebennikov *et al.*[56]). In the limit $IN(0) \gg 1$ this theory reduces to that of a Heisenberg antiferromagnet with an Anderson superexchange interaction. Furthermore, the results of this theory for the ground state at $T = 0$ and arbitrary values of $IN(0)$ agree with the results of the Hartree-Fock approximation for the Hubbard model.

In all the theoretical schemes mentioned, the description of the system of interacting electrons is based on the one-vertex Hubbard model. For describing "strong" itinerant magnets with more or less definite local moments these schemes are fully justified, and there is no doubt that the local spin fluctuations play the governing role. In the case of antiferromagnetic ordering, however, the weak point of theories of the local-spin-fluctuation type is that it is impossible to determine the type of magnetic lattice in a self-consistent manner. The magnetic superstructure must be put in artificially—for example, by dividing the lattice into two types of sites in the Hasegawa method.[52] This actually comes about because to describe the features of the band structure in the site representation one must keep a large number of off-diagonal (in the site indices) overlap integrals. This requires a detailed allowance for the intersite electron-electron correlations, a problem which is impractically complex in the local spin-fluctuation-theory.

We believe that the magnetic properties of almost all the known itinerant antiferromagnets are intimately related to features in their band structure. Specifically, the peculiar topology of the Fermi surface (the presence of nearly nested electron and hole portions) is responsible for the anomaly in $\chi(\mathbf{q})$. We realize the importance of taking collective excitations into account in general and in itinerant antiferromagnets in particular. However, analysis of the results of electronic-structure calculations for real itinerant antiferromagnets convince us that the aforementioned topological features of the Fermi surface are almost always an important factor in the formation of the antiferromagnetic ordering and must be taken into account to the same extent as spin-fluctuation effects.

In this review we shall not discuss "strong" antiferromagnets like γ-Fe and Mn, in which it is quite possible that well-defined local moments exist above the Néel point. It is for just such magnets that effects due to local spin fluctuations can be assumed to be most important, while an itinerant-magnetism approach in the spirit of SDWs does not apply at all. We will be talking about metals in which local moments are practically absent above the Néel point, i.e., the spin fluctuations are almost completely delocalized. These systems are "true" itinerant magnets, which are conveniently described in terms of the usual notions of an energy band structure. In many cases, no doubt, effects due to features of the band structure and effects due to spin fluctuations play equally important roles, but the theoretical description of this intermediate case has yet to be worked out.

The only pure metal that is an itinerant antiferromagnet in the sense described above is chromium, whose unique magnetic properties have traditionally aroused both theoretical and experimental interest. More than 500 papers have been written on this metal, and we must therefore limit our discussion mainly to the papers which have appeared in the last decade (and by no means all of these). The results of earlier studies are partially reflected in a number of reviews and quasi-reviews (see, e.g., Refs. 1 and 2) on the electronic structure and magnetic properties of chromium.

Neutron-diffraction measurements in single crystals have shown that the antiferromagnetic ordering in chromium differs substantially from the ordering in ordinary antiferromagnets. First, in pure chromium the antiferromagnetic structure is incommensurate with the body-centered cubic crystal lattice.[3] The wave vector of this structure is directed along one of the (100) axes, but its value is given by $Q = \left(\frac{2\pi}{a}\right)(1-\delta,\ 0,\ 0)$ (a is the lattice constant and $\delta = 0.048$–0.05[4]) and is weakly temperature dependent ($\delta = 0.037$ at $T \approx T_N$, where T_N is the Néel temperature). Second, these same measurements[5] have demonstrated that there are no localized magnetic moments whatsoever above the Néel temperature). The average magnetic moment per Cr atom is $0.46\mu_B$,[6] with the maximum magnetic moment being $0.59\mu_B$.[1)] The Néel temperature of pure Cr is 312 K, but below 120 K the transverse modulation of the magnetic moments gives way to a longitudinal modulation (a spin-flip transition). At the present time the nature of the spin-flip transition is not definitely decided; this effect is specific to Cr and does not occur in other systems discussed in this review, and so we shall not dwell on this question any further.

Interpretation of the magnetic properties of chromium (and its many alloys) from the standpoint of SDW theory has proved extremely fruitful. In this review we attempt to systematize all the results obtained in this area, most of which are based on the "excitonic insulator" model. This model is discussed in detail in Sec. 2. It must be noted that most of the experimental results—the concentration phase diagrams of chromium aloys, the transition from incommensurate to commensurate structure, the change in the magnetic structure and properties under pressure, the anomalies in the optical properties, kinetic effects, the behavior of the magnetic susceptibility, etc.—find a good qualitative, and in some cases semiquantitative (see, e.g., Sec. 3) description in terms of this theoretical model.

Table I gives some experimental results from Ref. 7 which show the influence of different transition-metal im-

[1)]An isolated chromium ion can have a moment as high as $3\mu_B$.

TABLE I. Properties of alloys of Cr with d transition metals[7]

Impurity	V	Mo	W	Mn	Fe	Co	Ni
N_e	−1	0	0	1	2	3	4
$\left(\frac{\Delta Q}{\Delta c}\right)\cdot\frac{2\pi}{a}\cdot 10^{-3}$	−15	0	0	15	7	10	−8
N_d	−1	0	0	1	0.5	0.7	−0.6
μ_i	0	0	0	0	1,5	2.0	0
ΔT_N (in K) at 0.5%—experiment	−62	−7	−10,5	77	−12	−18	−75
ΔT_N (in K) at 0.5%—rigid-band	−70	0	0	70	35	49	−52

N_e is the number of excess d electrons, N_d is the number of d electrons entering the d band of Cr per impurity atom; μ_i is the local moment per impurity atom; c is the concentration of the impurity.

purities on the vector **Q** and the Néel temperature. A detailed survey of the phase diagrams of dilute alloys of chromium with transition metals has been given by Butylenko and Kobzenko.[8] Also given in Table I are the results of a calculation of the change in T_N in the rigid-band approximation. It is seen that the rigid-band approximation is entirely satisfactory for alloys with V and Mn and somewhat satisfactory for Ni and that effects due to scattering by isoelectronic impurities are relatively small (alloys with Mo and W), but also that the rigid-band model is absolutely unsuitable for alloys with ferromagnetic $3d$ metals having local magnetic moments (Fe and Co). This approximation also fails to describe alloys with nontransition metals (Al, Ge, Si, Ga, Sb).

The completely unusual form of the phase diagrams of alloys of chromium with nontransition metals (CrSi and CrAl, for example) and the anomalies of the kinetic effects and magnetic properties of the alloy CrFe do not fit into the existing theoretical concepts (or, possibly, these results have been interpreted incorrectly). The problem of interpreting certain neutron-diffraction measurements in incommensurate structures is also far from solved, for the reason that no theory has been developed to describe the collective excitations in structures of this kind.

Although the material reviewed mainly illustrates the application of the theory of the SDW instability to the physical properties of chromium and its dilute alloys, there are also other metallic systems which exhibit a transition to a SDW state. Such substances include vanadium sulfides and selenides (V_3S_4, V_3Se_4, V_5S_8, V_5Se_8), chromium diboride (CrB_2), an intermetallic compound from the group of the Laves phases of $TiBe_2$, the helical magnet MnSi, and a number of other metals. However, the physical properties of these substances are not as well studied, and one of our goals in this review is to call these systems to the attention of researchers.

2. THE "EXCITONIC INSULATOR" MODEL—THE BASIS FOR THE THEORETICAL DESCRIPTION OF THE SPIN-DENSITY-WAVE STATE

In 1962, Overhauser[10] showed that the paramagnetic ground state of a homogeneous electron gas in the Hartree-Fock approximation is unstable with respect to the formation of a SDW. Generally speaking, the instability vanishes when the screening of the exchange and Coulomb interactions is taken into account.[11] However, band-structure effects can stabilize the SDW state,[12,13] as happens in chromium, for example.

The most suitable model for quantitative description of the transition to the SDW state is the "excitonic insulator" model proposed by Keldysh and Kopaev[14] (see also Halperin and Rice,[15] de Cloizeaux,[16] and Kozlov and Maksimov[17]). In this model one considers interacting electrons and holes whose dispersion relation has the property

$$\varepsilon_1(\mathbf{k}) = -\varepsilon_2(\mathbf{k}+\mathbf{Q}). \tag{2}$$

Equation (2) is satisfied for a rather large number of vectors **k** lying near the Fermi surface. In a three-dimensional system such a situation is possible, for example, if the electron and hole Fermi surfaces are spherical or have nested portions.

In the excitonic insulator model there are four possible types of phase transitions[15,18]: transitions to SDW and CDW states characterized by real order parameters, and transitions to two states with imaginary order parameters. The Hamiltonian of the excitonic insulator model is of the form[19]

$$\begin{aligned} H = &\sum_{i,\mathbf{k},\sigma} \varepsilon_i(\mathbf{k})\, a^\dagger_{i\sigma}(\mathbf{k})\, a_{i\sigma}(\mathbf{k}) \\ &+ \sum_{\mathbf{k},\mathbf{k}',\mathbf{q},\sigma,\sigma'} [g_1 a^\dagger_{1\sigma}(\mathbf{k})\, a^\dagger_{2\sigma'}(\mathbf{k}')\, a_{2\sigma'}(\mathbf{k}'+\mathbf{q}) \\ &\times a_{1\sigma}(\mathbf{k}-\mathbf{q})] \\ &+ g_2[a^\dagger_{1\sigma}(\mathbf{k})\, a^\dagger_{1\sigma'}(\mathbf{k}')\, a_{2\sigma'}(\mathbf{k}'+\mathbf{q})\, a_{2\sigma}(\mathbf{k}-\mathbf{q}) + \text{c.c.}] \\ &+ g_2[a^\dagger_{1\sigma}(\mathbf{k})\, a^\dagger_{2\sigma'}(\mathbf{k}')\, a_{1\sigma'}(\mathbf{k}'+\mathbf{q})\, a_{2\sigma}(\mathbf{k}-\mathbf{q}) + \text{c.c.}] \\ &+ \lambda_{12} \sum_{\mathbf{k},\sigma,\mathbf{q}} u_{\mathbf{q}}[a^\dagger_{1\sigma}(\mathbf{k})\, a_{2\sigma}(\mathbf{k}-\mathbf{q}) + \text{c.c.}] + \sum_{\mathbf{q}} \omega_{\mathbf{q}} b^\dagger_{\mathbf{q}} b_{\mathbf{q}}; \end{aligned} \tag{3}$$

here $a^\dagger_{1,2}$ and $a_{1,2}$ are the creation and annihilation operators for electrons and holes in bands 1 and 2, respectively, g_1 is the constant for the interband screened Coulomb interaction of the density-density type, g_2 is the interaction constant describing the interband transition of a pair of particles, λ_{12} is the interband electron-phonon interaction constant, $\omega_{\mathbf{q}}$ is the bare phonon frequency, and $u_{\mathbf{q}}$ is the displacement operator for the ion. For simplicity, all the constants in the exci-

tonic insulator model are assumed to be independent of the momenta (we assume an effective averaging over angles on the Fermi surface), i.e., the interactions are assumed to be of short range.

The transition to the SDW state is characterized by an effective constant $g_t = g_1 + g_2$, the transition to the CDW state by the constant

$$g_s = g_1 + g_2 + 4\left(\frac{\lambda_{12}^2}{\omega_Q} - g_2\right).$$

For a weak electron-phonon interaction $\lambda_{12}^2/\omega_Q < g_2$ the SDW state (for $g_2 > 0$) is the most favorable, since it corresponds to a larger interaction constant and a higher transition temperature T_N. It is this case which we shall consider below. The states with imaginary order parameters are less favorable than the SDW state, since they correspond to an effective constant $g_{Im} = g_1 - g_2$. We shall not consider these states below. A detailed analysis of the interaction constants in the excitonic insulator model was recently given by Buker.[20]

The excitonic insulator model admits an asymptotically exact solution for $gN(0) \ll 1$ ($N(0)$ is the reduced density of states at the Fermi surface). This solution is obtained in mean field theory,[19] and the corresponding mathematical apparatus is analogous to Gor'kov's method in the theory of superconductivity.[21] We shall consider in detail the case of the so-called commensurate (doubled) antiferromagnetic structure, for which $\mathbf{Q} = +\mathbf{G}/2$, where $\mathbf{G}$ is a reciprocal lattice vector of the crystal.

In the mean field approximation one can go over from Hamiltonian (3) to an effective Hamiltonian for electrons moving in an exchange field Δ_t with components $\Delta_{ij}^{\alpha\beta}(\mathbf{q}) = \Delta_{t\mathbf{q}}\hat{\sigma})_{ij}^{\alpha\beta}$:

$$H_{eff} = H_0 - \sum_{\alpha,\beta,\mathbf{k},\mathbf{q},i,j} (\Delta_{t\mathbf{q}}\hat{\sigma})_{ij}^{\alpha\beta} a_{i\alpha\mathbf{k}+(\mathbf{q}/2)}^{+} a_{j\beta\mathbf{k}-(\mathbf{q}/2)} + \frac{1}{g_t}\sum_{\mathbf{q},\alpha,\beta,i,j} (\Delta_{t\mathbf{q}}\hat{\sigma})_{ij}^{\alpha\beta} (\Delta_{t,-\mathbf{q}}\hat{\sigma})_{ji}^{\beta\alpha}. \quad (4)$$

The self-consistency equation for $T = 0$ can be obtained by variation of (H_{eff}) with respect to the parameter $\Delta_{ij\mathbf{q}}^{\alpha\beta}$. At a finite temperature one should vary not the energy but the free energy F corresponding to (4). The self-consistency equation in this case is expressed in terms of a sum over imaginary frequencies

$$\omega_n = \pi T(2n+1), \quad n = 0, \pm 1, \ldots, \quad (5)$$

$$\Delta_{12\mathbf{q}}^{\alpha\beta} = g_t T \sum_{n,\mathbf{k}} G_{12}^{\alpha\beta}(k, \mathbf{q}, \omega_n), \quad (6)$$

where $G_{12}^{\alpha\beta}(\mathbf{k}, \mathbf{q}, \omega_n)$ are the temperature Green functions.

One can show that in the case of a linearly polarized sinusoidal antiferromagnetic structure the choice $\mathbf{q} = \pm\mathbf{Q}$ exactly satisfies the self-consistency equation. In this case

$$\Delta_{ij,\pm\mathbf{Q}}^{\alpha\alpha} = -\Delta_{ij,\pm\mathbf{Q}}^{-\alpha,-\alpha} = \Delta_{t,\pm\mathbf{Q}}\sigma^z \quad (7)$$

and the direction of the local magnetization vector $\mathbf{m}(\mathbf{r})$ (or, equivalently, $\Delta_{t\mathbf{Q}}$) is chosen along the quantization axis z.

We note that Eq. (7) is by no means the only possible magnetic structure described by Hamiltonian (3).

Right now we are interested only in a sinusoidal linearly polarized SDW with $\mathbf{q} = \pm\mathbf{G}/2$, in which case for $\Delta_{t,\pm\mathbf{Q}} \neq 0$ there is a doubling of the magnetic period of the crystal in the direction of the vector $\mathbf{G}$.

Let us now return to the problem of calculating Δ_t. Keeping in mind that we shall be applying the result to real metals with a SDW, we must allow for the possibility that the electron and hole surfaces may not coincide, as is actually always the case. The simplest way to do this is to introduce the momentum-independent quantity μ_0, which has a clear physical meaning. Suppose for simplicity that the dispersion relations of electrons in bands 1 and 2 are isotropic, i.e.,

$$\varepsilon_1(\mathbf{k}) = \frac{k^2}{2m^*} - \varepsilon_{F_1}, \quad (8)$$

$$\varepsilon_2(\mathbf{k}-\mathbf{Q}) = -\frac{k^2}{2m^*} + \varepsilon_{F_2}; \quad (9)$$

where m^* is the effective mass, $m_1^* = m_2^* = m^*$, but we can also consider a more general situation. Introducing the quantities $2\mu_0 = \varepsilon_{F_1} - \varepsilon_{F_2}$ and $2\varepsilon_F = \varepsilon_{F_1} + \varepsilon_{F_2}$, we arrive at the following notation:

$$\varepsilon_1(\mathbf{k}) = \zeta_{\mathbf{k}} - \mu_0, \quad (10)$$

$$\varepsilon_2(\mathbf{k}-\mathbf{Q}) = -\zeta_{\mathbf{k}} - \mu_0, \quad \zeta_{\mathbf{k}} = \frac{k^2}{2m^*} - \varepsilon_F, \quad (11)$$

i.e., μ_0 plays the role of a chemical potential.

We shall not go through the derivation of the BCS-type equation for the order parameter Δ_t but shall refer the reader to the detailed paper of Kopaev.[19] This equation is of the form

$$\Delta_t = g_t N(0) \int_0^W \frac{\Delta_t}{2\tilde{\varepsilon}_{\mathbf{k}}}\left(\operatorname{th}\frac{\tilde{\varepsilon}_{\mathbf{k}}+\mu}{2k_BT} + \operatorname{th}\frac{\tilde{\varepsilon}_{\mathbf{k}}-\mu}{2k_BT}\right) d\zeta_{\mathbf{k}}, \quad (12)$$

$$\tilde{\varepsilon}_{\mathbf{k}} = \sqrt{\zeta_{\mathbf{k}}^2 + \Delta_t^2}. \quad (13)$$

The quantity μ in (12) is generally not equal to μ_0, since the chemical potential of the system changes because of the change in the electron spectrum (in proportion to Δ_t^2) in such a way that the total number of particles is conserved and does not depend on Δ_t. The effective cutoff energy W of the Coulomb interaction is a parameter of the model. It is more convenient, however, to transform to the universal energy-scale characteristic

$$\Delta_0 = 2W\exp\left[-\frac{1}{g_t N(0)}\right], \quad (14)$$

which is the solution of (12) for $T = 0$, $\mu = 0$. It is also convenient to introduce the universal temperature characteristic

$$\mathring{T}_N = 0.57\Delta_0, \quad (15)$$

which is the temperature of the transition to the SDW state when the Fermi surfaces are perfectly coincident ($\mu = 0$).

Assuming that the phase transition to the SDW state is second order, we obtain from (12) an equation for the Néel temperature T_N. Dividing both sides of the equation by Δ_t and setting $\Delta_t = 0$ and $\mu = \mu_0$ in the resulting expression, we get

$$-\ln\frac{T_N}{\mathring{T}_N} = \operatorname{Re}\left[\Psi\left(\frac{1}{2} + i\frac{\mu_0}{\pi k_B T_N}\right) - \Psi\left(\frac{1}{2}\right)\right], \quad (16)$$

where $\Psi(x)$ is the digamma function.

Solution (16) was obtained by Rice[22] and Kopaev.[23]

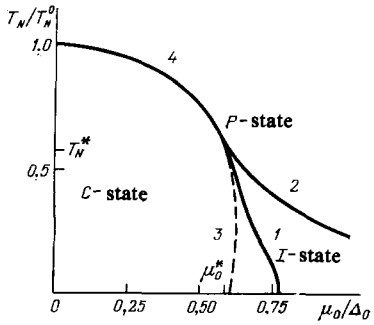

FIG. 1. Phase diagram of the excitonic insulator model. 1) the line of the transition to the I phase in Rice's model[22]; 2) the line of the transition to the I phase in the octahedral model[90]; 3) the line of the I-C transition in the octahedral model[90]; 4) the line of the transition from the P phase to the C phase.

This solution is represented graphically in Fig. 1. The line $T_N(\mu_0)$ bounds the region of the commensurate (C) phase. One notices that the curve $T_N(\mu_0)$ is double-valued for $\mu_0 > \Delta_0/2$. Rice[22] has shown that at sufficiently large $\mu_0 > \mu_0^*$ ($\mu_0^* \approx 0.604\ \Delta_0$) there is in fact an incommensurate SDW structure whose wave vector does not coincide with G/2. The $T_N(\mu_0)$ phase diagram exhibits a tricritical point ($T_N^* \approx 0.31\ \Delta_0$, $\mu_0^* \approx 0.604\ \Delta_0$) at which the lines of transitions between the paramagnetic (P) phase and the antiferromagnetic C and antiferromagnetic incommensurate (I) phases and the line of transitions between the C and I phases all come together.

The incommensurate SDW structure and the phase diagram in various models of the spectrum will be analyzed in a separate section of this review. The line shown in Fig. 1 for the transition from the P to the I phase was found by Rice under the assumption that the P-I transition is second order. Although this assumption has turned out to be incorrect, the P-I transition line in Fig. 1 nevertheless gives a tentative idea of the existence region of the I phase. The C-I transition line was not found by Rice and apparently cannot be obtained correctly in his model.

We should say a few words about the chemical potential μ in (13). The chemical potential is defined by the condition that the total number of particles in the system is conserved. We assume that in addition to the nested portions of the spectum, $\varepsilon_1(\mathbf{k})$ and $\varepsilon_2(\mathbf{k})$, there are also other bands which are not anomalous and do not participate in the formation of the SDW wave; the average density of states for these bands at the Fermi surface is $N_r(0)$. In this case[22] the condition of conservation of the number of particles can be written

$$\delta n(\mu) + N_r(0)(\mu - \mu_0) = 0, \tag{17}$$

where

$$\delta n(\mu) = 2N(0)\int_0^\infty d\zeta_{\mathbf{k}}\{[n(\tilde{\varepsilon}_{\mathbf{k}} - \mu) + n(-\tilde{\varepsilon}_{\mathbf{k}} - \mu)] - [n(\zeta_{\mathbf{k}} - \mu_0) + n(-\zeta_{\mathbf{k}} - \mu_0)]\} \tag{18}$$

and $n(x)$ is the Fermi function.

If $N_r(0) \ll 2N(0)$, then the chemical potential μ can be strongly affected by the appearance of the SDW ($\Delta_t \neq 0$), and Eq. (17) must be solved jointly with (13). If, on the other hand, $N_r(0) \gg 2N(0)$, then the difference between μ and μ_0 can be neglected [it is of relative order β^{-1}, where $\beta = N_r(0)/2N(0)$]; in Rice's terminology[22] β is called the "capacity of the electron reservoir". In real SDW systems the parameter β can have any value (for example, in chromium $\beta \sim 1$), but all the qualitative results of the excitonic insulator model can be obtained in the limiting cases $\beta = 0$ and $\beta = \infty$ (i.e., $\mu = \mu_0$).

The assumption $\beta = \infty$ usually leads to results which are closer to reality than in the opposite limit $\beta = 0$. This circumstance is due to allowance for the influence of that portion of the Fermi surface of the metal which is not involved in the formation of the SDW; this portion of the Fermi surface is generally large.

Still another complication which must be introduced into the simple excitonic insulator model is scattering by impurities. In the case of an alloy there are two effects that must be taken into account: scattering by impurities, and the change in the chemical potential μ_0 (the latter is always present except in the case of isoelectronic impurities such as Mo and W in Cr). The effect of nonmagnetic-impurity scattering on the phase transitions in the excitonic insulator model was studied by Zittartz[24] and Kopaev *et al.*[25]

To Hamiltonian (3) we must add the term

$$H_{\text{imp}} = \sum_{\mathbf{k},\mathbf{q},i,j,\alpha} U^{ij}(\mathbf{q})\, a_{i\alpha}^+(\mathbf{k})\, a_{j\alpha}(\mathbf{k}+\mathbf{q}), \tag{19}$$

$$U^{ij}(\mathbf{q}) = \sum_m \int \varphi_{i\mathbf{k}}^*(\mathbf{r})\, U(\mathbf{r} - \mathbf{R}_m)\, \varphi_{j,\mathbf{k}+\mathbf{q}}(\mathbf{r})\, d\mathbf{r}, \tag{20}$$

where m is the number of the site at which the impurity is located and $U(\mathbf{r} - \mathbf{R}_m)$ is the impurity potential. One usually considers only intraband components $U^{ij}(\mathbf{q})$ and thereby simplifies the problem, but in general the interband components of the type $U^{12}(\mathbf{q})$ do not contain a small factor.[25]

Taking into account only the intraband scattering by a nonmagnetic impurity in the Born approximation, one can obtain the following equation for the temperature of the transition to the C phase:

$$-\ln\frac{T_N}{\mathring{T}_N} = \operatorname{Re}\left[\Psi\left(\frac{1}{2} + i\frac{\mu_0}{2\pi k_B T_N} + \frac{1}{4\pi\tau k_B T_N}\right) - \Psi\left(\frac{1}{2}\right)\right], \tag{21}$$

where $1/2\tau = c\pi N(0)\langle(U^{ii})^2\rangle$ is the reciprocal relaxation time of the momentum in the scattering of an electron by the impurity (for simplicity $U^{11} = U^{22}$). One can also include phonon scattering in τ and thereby allow for temperature dependence of $\tau(T)$. In the limit of very low impurity concentrations $c \ll 1$ and for $\mu_0 = 0$ one can easily obtain[25]

$$-\ln\frac{T_N}{\mathring{T}_N} = \frac{\pi}{4\tau k_B T_N}, \tag{22}$$

i.e., in the simplest approximation impurity scattering decreases the transition temperature in comparison with the case of the pure metal. The influence of impurity scattering on the transition to the I phase is of approximately the same order of magnitude as estimate (22).

There are a number of rather subtle effects due to the appearance of local impurity states in the excitonic insulator model. In essence, these effects are intimately related to fundamental questions pertaining to the metal-insulator transition in disordered systems. Here there are still many un-

solved problems concerning, in particular, the gapless regime, resonant localized states near a defect, local rearrangement of the charge and spin densities, etc. Unfortunately, a detailed discussion of these questions is beyond the scope of this review.

An interesting problem is to allow for the temperature dependence of τ. Since the actual temperature T_N in certain SDW systems is not small compared to the Debye temperature (e.g., in chromium $\theta_D \approx 630$ K, $T_N \approx 312$ K), allowance for phonon scattering can appreciably alter T_N. Fenton and Leavens[26] have attempted to incorporate this effect in the framework of the Eliashberg method, which was originally developed for semiconductors (see Ref. 27). In Ref. 28 the present authors questioned the radical change (by about a factor of five) that was obtained numerically in Ref. 26: analysis of the corresponding terms in the Eliashberg equation showed that in the two-band model the electron-phonon scattering processes considered in Refs. 26 and 28 could not change T_N by very much for a reasonable choice of electron-phonon interaction constants. However, this does not rule out the possibility of an appreciable change in T_N, since the function $\tau(T)$ in (21) is determined by all the electrons near the Fermi surface and, to a considerable degree, by the electrons of the reservoir. We believe that it is entirely sufficient to include this dependence directly in (21), as was done, for example, in Ref. 29.

3. ANTIFERROMAGNETISM IN CHROMIUM AND ITS ALLOYS: EXPERIMENT

Dilute alloys of chromium with various metals are promising objects for comparison of experiment with the theory of the excitonic insulator. Alloys with nonmagnetic transition metals can be described qualitatively by the rigid-band model, and the change in concentration can thus be modeled by a change in the parameter μ_0 (e.g., alloys of chromium with Mn, V, Re, Os, etc.). On the other hand, as we have mentioned, scattering by impurities also affects the antiferromagnetic structure and Néel temperature. However, for nonmagnetic impurities which are nonisoelectronic this effect is rather small in comparison with the effect of the change in the position of the chemical potential. At the same time, for Mo and W, which are isoelectronic with Cr, impurity scattering is solely responsible for the changes in the SDW parameters.

The chromium alloys which are adequately described in the rigid-band model can be divided into two types, according to whether the impurity metal stands to the right or left of Cr in the periodic table. In the first case the position of the chemical potential rises with increasing impurity concentration on account of the increase in the electron density. This tends to equalize the volumes of the Fermi surfaces for the electrons and holes (see Sec. 4 below), increases $\tilde{\mathbf{Q}}$, i.e., decreases $\tilde{\delta}$, so that at a certain impurity concentration a perfect antiferromagnetic structure arises in the alloy, with a magnetic superlattice of the CsCl type. In such alloys the SDW is commensurate with the crystal lattice and has a wave vector $\mathbf{Q} = (2\pi/a)(1,0,0)$.

For example, in the alloy CrRe it is found[30] that as the

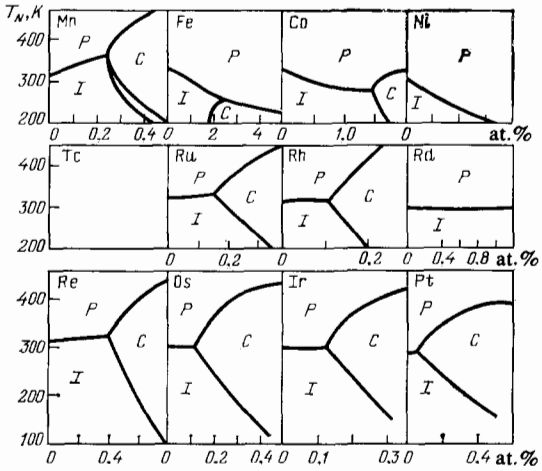

FIG. 2. Portions of the phase diagrams of alloys of chromium with transition metals.[31] There are no data for CrTc.

Re concentration is increased from 0 to 0.8 at. % the wave vector $\mathbf{Q}$ increases with temperature and concentration up to a critical value $0.97 \cdot 2\pi/a$ and then abruptly jumps to $2\pi/a$. Here the transition between the commensurate and incommensurate phases occurs in a certain interval of concentrations, i.e., it has a temperature boundary such that the high-temperature phase which arises from the paramagnetic state is commensurate, while the low-temperature phase is incommensurate. Since the transition in pure chromium occurs directly between the P and I phases, the phase diagram of the alloy should have a tricritical point. Figure 2 gives examples of phase diagrams of dilute alloys of Cr with various transition metals.[31]

It is seen from Fig. 2 that all diagrams of group-I alloys (nonmagnetic metals of high valence) have a triple point and at sufficiently high impurity concentrations exhibit a commensurate antiferromagnetic phase. On the other hand, grou-II alloys (metals of lower valence) have phase diagrams characterized by the presence of only the I phase, whose Néel temperature falls off rapidly with increasing impurity concentration. The isoelectronic alloys CrMo and CrW behave in a similar manner, but the rate of decrease of T_N here is much slower, since the decrease is due solely to scattering effects.

The most detailed neutron-diffraction study of chromium alloys with nonmagnetic transition metals was carried out by Koehler *et al.*[32] It was found that the average magnetic moment per atom for group-II alloys falls off with increasing impurity concentration at almost the same rate as does the Néel temperature, while for group-I alloys it increases, passes through a maximum, and then remains practically constant (Fig. 3). Accordingly, in group-II alloys the magnitude of $\mathbf{Q}$ also decreases with increasing concentration. Figure 4 shows the dependence of $\mathbf{Q}$ on the composition of the alloy for two temperatures ($T \approx T_N$ and $T \ll T_N$). It is seen that $\mathbf{Q}$ also falls off in isoelectronic alloys, but at a much slower rate than in CrV alloys.

It is now well established that in pure Cr the transition at T_N is of first order. This fact has been made clear by measurements of the coefficient of thermal expansion, the

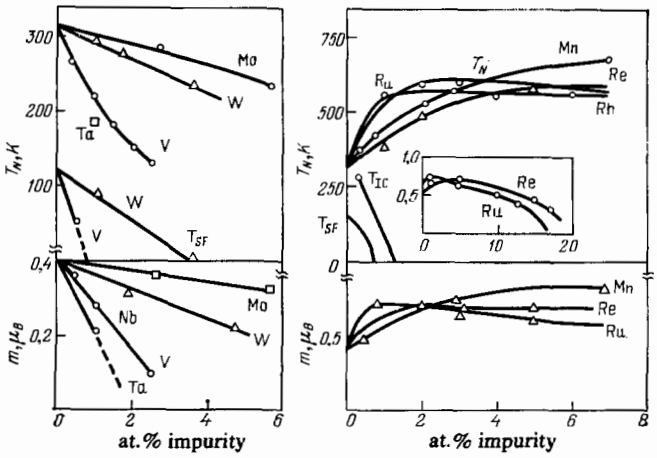

FIG. 3. Transition temperature and spontaneous moment for chromium alloys, according to the data of Ref. 32. Also plotted are the temperature T_{SF} of the spin-flip transition and the temperature T_{IC} of the transition between the incommensurate and commensurate phases.

compressibility, the specific heat, and other thermodynamic characteristics (see the literature cited in Ref. 33). However, it must be stressed that this transition is extremely close to second order. For example, the entropy of transition is only 0.19 cal/mole, and the relative change in volume at the transition is between $5 \cdot 10^{-4}$ and $3 \cdot 10^{-4}$. Such quantities are usually considered negligible in identifying the order of the transition.

In very dilute alloys of chromium with group-I metals and in alloys with group-II metals the transition remains first order.[33] For example, in CrRe alloys it has been found[30] that at very low Re concentrations the transition is first order, but at higher concentrations ($\sim$0.7 at. %), at which the transition is from the P phase to the C phase, the order of the transition is unclear, but it is extremely close to second order.

The most detailed study of the order of the transition between the I and C phases was recently carried out[33] for CrMn alloys, in which this transition is observed at concentrations between 0.3 and 1.1 at. % Mn. Studies have been done at compositions in this range by the methods of neutron diffraction,[32–35] magnetic susceptibility,[34] thermal expansion,[33,36] electrical resistance,[33,38] and specific heat.[33,37] The presence of a large hysteresis indicates that the transition is of first order. However, the transition at T_{IC} is in itself not very sharp, and in certain cases the width of the transition is greater than the hysteresis. This can be interpreted in two ways: 1) as evidence of coexistence of the C and I phases in a certain temperature interval,[34,36] and 2) as evidence of inhomogeneity in the Mn distribution over the sample.[39]

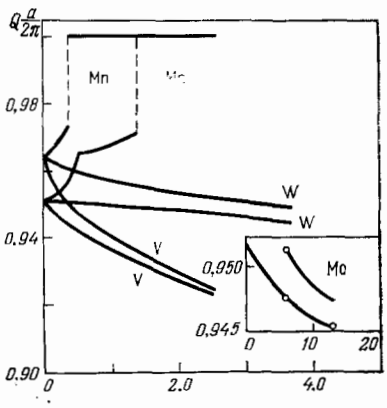

FIG. 4. SDW wave vector as a function of the composition for chromium alloys.[32] The value $Q = 2\pi/a$ corresponds to a commensurate structure. The upper curves refer to measurements made near T_N; the lower curves are for low temperatures.

A study of CrMn samples of homogeneous and inhomogeneous composition has led to the conclusion[33] that the model which assumes coexistence of the I and C phases is not supported by experiment. Measurements were made of neutron diffraction, thermal expansion, resistance, and specific heat. A latent heat of transition was found, i.e., it was clearly established that the transition at T_{IC} is of first order.

Thus we see that alloys of Cr with metals of groups I and II have phase diagrams which are described completely by the excitonic insulator model. An important test of the applicability of the theory is the behavior of these alloys under pressure. The first measurements of T_N under pressure in pure Cr were done by neutron-diffraction[43] and ultrasonic[44] methods. It was found that T_N decreases under pressure at an enormous rate (-6.0 K/kbar in Ref. 43 and -5.6 K/kbar in Ref. 44) which is not proportional to the compressibility. In another study[45] done at almost the same time the pressure was varied up to 8 kbar, and T_N was found to decrease at a rate of -5.1 K/kbar.

By now the behavior of T_N under pressure has been studied in almost all dilute alloys of chromium. Group-I alloys (CrRe, CrMn, CrRu) were studied in Ref. 46, where it was shown that in the I phase T_N also has a slope close to -5 K/kbar, while in the C phase the change in T_N under pressure is even faster. It was also shown that a transition from the C phase to the I phase occurs under pressure. In Ref. 38 it was also found that pressure inhibits the formation of the C phase (at least at concentrations up to 4 at. % Mn). An analogous effect of pressure has been found[47] for CrOs alloys, and a study[48] of the isoelectronic alloy CrMo at pressures up to 3 kbar has also revealed a weak decrease in dT_N/dP with increasing Mo concentration.

The effect of pressure in alloys of Cr with group-II metals (CrV) was investigated in Ref. 49. Here it was shown that dT_N/dP is a universal linear function of T_N (in the I phase). This means that measurements of dT_N/dP in CrV as a function of the concentration lie on the same straight line as do measurements[50] of dT_N/dP in pure Cr at pressures up to 85 kbar (Fig. 5). McWhan and Rice[50] have demonstrated that the experimental pressure dependence $T_N(P)$ is described well by the formula

$$\ln \frac{T_N}{T_N(0)} = C\,\frac{\Delta V}{V_0}, \tag{23}$$

where $C = (B_0/T_N(0))(dT_N/dP)_0 = -26.5$, $(dT_N/dP_0) = -5.1$ K/kbar, and $T_N(0) = 3.12$ K. These results are shown in Fig. 6. The rate of decrease of T_N under pressure thus slows substantially with increasing pressure.

If it is assumed that T_N is described by the formula from the excitonic insulator theory in the limit $\mu = 0$, i.e., (16), while the change of the effective constant with pressure is

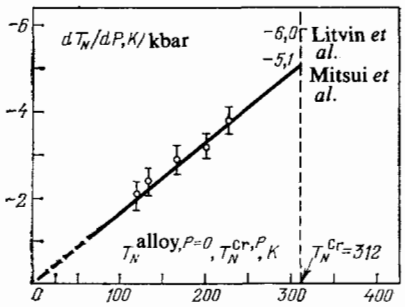

FIG. 5. Pressure derivative $dT_N dP$ as a function of T_N for CrV alloys in the limit $P \to 0$. The straight line shows the results of measurement under pressure[50] for pure chromium, while the points are experimental data [49] for CrV with different impurity concentrations. Also shown are the values of $dT_N dP$ obtained for pure Cr in the limit $P \to 0$.

proportional to the volume change $\Delta V / V_0$, then dependence (23) is obtained immediately.

Thus the excitonic insulator theory exactly predicts the functional dependence of the Néel temperature on pressure. The larger absolute value of dT_N/dP in the C phase is evidently due not only to a decrease in the effective interaction constant but also to an increase in μ_0 with pressure [the influence of μ_0 is not taken into account in (23)]. This factor stabilizes the I phase under pressure, in accordance with the equation of state of the excitonic insulator model.

There is considerable interest in the unusual phase diagrams of alloys of chromium with nontransition elements; these diagrams cannot be described in terms of the simple excitonic insulator model used above. At the present time there is no consistent theoretical interpretation of the properties of these alloys. Let us briefly discuss the main experimental facts.

One of the most interesting alloys of this group is **CrAl**. The unusual phase diagram of this alloy is shown in Fig. 7.[54] Recent precision measurements of the electrical resistance $R(T)$ and the magnetic susceptibility $\chi(T)$[53–55] with changing temperature, concentration, and pressure have shown that for $x < 1.1\%$ the temperature $T_N(x)$ falls off at a rate $dT_N/dx \approx -60$ K/at. %, for $1.1 < x < 3\%$ it falls at -120 K/at. %, and for $x > 3\%$ it rises at a rate of 300 K/at. %. In measurements under pressure there is a sharp increase in the pressure derivative dT_N/dP for $x > 1.2\%$ (from -7 K/kbar at $x = 1.2\%$ to -25 K/kbar at $x = 2\%$), whereas in the interval $0 < x < 1.2\%$ the pressure derivative changes very little. In this same concentration region the vector **Q** of the SDW remains practically unchanged, but at the transition to the C phase it goes practically discontinuously to $2\pi/a$. In addition, for $x > 1.2\%$ there are flat but readily noticeable minima on the static magnetic susceptibility $\chi(T)$ in the paramagnetic region ($T_{min} \approx 600$ K).

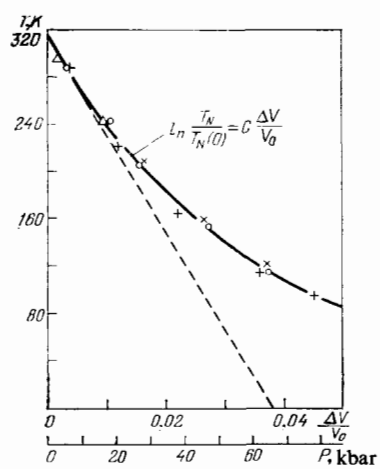

FIG. 6. Néel temperature of chromium versus the atomic volume. The experimental points[50] are described well by an exponential curve.

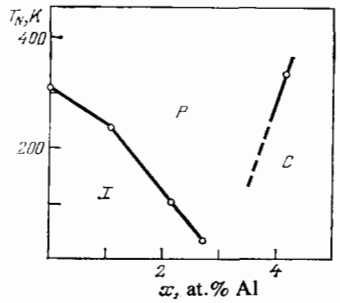

FIG. 7. Curve of $T_N(x)$ for the alloy CrAl.[54]

The isoelectronic phase diagram of the alloy **CrGa**[57] is extremely similar to the diagram of **CrAl**, but here the minimum of T_N is less sharp. At the same time the phase diagram of the alloy **CrSi** (Fig. 8) differs from the diagrams considered earlier in that here all the phase transitions are first order. The first order character of the transition from the P phase to the C phase for $x > 1$ at. % Si is demonstrated not only by measurements of the electrical resistance, susceptibility[61], and thermoelectromotive force,[62] but also by direct measurements of the latent heat of transformation.[58] Very complex behavior is observed for **CrSi** under pressure. Neutron diffraction[66,67] has revealed that for $x < 1.0\%$ and at pressures up to 5 kbar the I phase of the SDW remains stable, although there is a slight decrease in T_N that can be attributed to an increase in μ_0 with pressure. For $x > 1.0\%$, however, there is initially (in the C-phase region) a decrease in T_N, and at pressures $p > 1$ kbar ($x = 1.4\%$) there is a rapid increase in the complexity of the phase diagram, with a succession of transitions (on decreasing temperature) first to the I phase

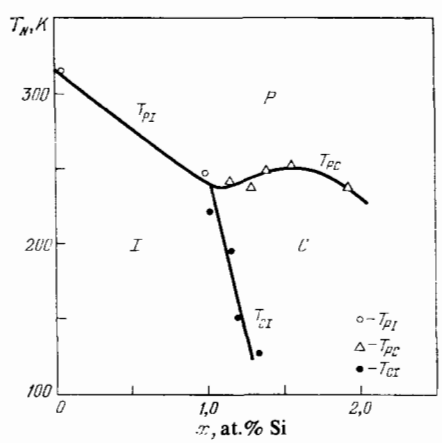

FIG. 8. Phase diagram for the alloy CrSi.[64] The transition at T_{PC} is first order.

and then to a mixed phase I + C, and, when the pressure is increased to 2–3 kbar, to the C phase as well. The behavior of the vector **Q** of the SDW in this concentration region is also very complex. In the I-phase region ($x < 1\%$) **Q** increases with increasing x, i.e., there is a tendency toward transition to the C phase. Jayaraman *et al.*[60] conjectured that this is evidence that silicon has a donor character in chromium, under the assumption that silicon is an interstitial impurity.

The decrease in T_N here should be due solely to the effect of scattering, since there would be a decrease in μ_0 that should increase T_N. Recent neutron-diffraction studies[65] have shown that the Si atoms (like Al) are located at chromium lattice sites, and therefore the donor behavior of Si cannot be attributed to its interstitial location.

It is clear that the simple two-band model cannot explain all the features of the unusual diagrams shown in Figs. 7 and 8. While in the case of **CrSi** the assumption of a donor character of the impurity and the use of the excitonic insulator model with allowance for scattering by impurities and phonons and the presence of a reservoir[102] enabled Benediktsson *et al.*[58] to link the first-order character of the P-C phase transition to the influence of magnetostriction, in the case of **CrAl** there is a clear indication of a change in the electronic state of the impurity at the transition from the I phase to the C phase. It can be assumed that a local bound state forms near the Al atom in the Cr lattice, and at low concentrations the Al atoms act like uncharged impurities on the state of the I phase. If it is assumed that the level becomes quasiresonant upon an increase in x, the sharp increase in scattering would cause T_N to fall off rapidly, and the SDW state could vanish entirely. With further increase in x the local level would rise above the Fermi energy, i.e., the Al would become a donor impurity and the resonant character of the scattering would vanish. These two factors would tend to increase T_N and to stabilize the C phase of the SDW.

In the case of the alloy **CrGe** the phase diagram is analogous to that of **CrMn** (Fig. 9).[68,69] In the I-phase region the vector **Q** increases with increasing x, and on the I-C transition line it jumps abruptly to $2\pi/a$.[70] In the C-phase region the magnetic moment (as for Al, but unlike the case of Si) increases slightly with increasing x. From this it can be conjectured that the local level in **CrGe** is above the Fermi level right from the start, and that Ge is a donor in this alloy. This conjecture is confirmed by neutron-diffraction measurements under pressure.[71] A completely analogous situation exists in **CrSb**.[72]

In **CrBe**[73] the C phase is not observed at all, and T_N falls off slowly with increasing x; this is evidently due to ordinary scattering of the SDW by defects. We note that Be, unlike the nontransition elements discussed earlier, does not have p-type valence electrons. It is possible that the p orbitals are responsible for the formation of the local level.

A still more complex situation arises in the dilute ($x < 5\%$) alloys **CrCo** and **CrFe**, in which the impurity atoms clearly have an intrinsic local magnetic moment. At the present time we do not have a consistent theory explaining all the unusual properties of these alloys. We believe that the features of the phase diagrams of **CrCo** and **CRFe** (see Fig. 2) are not in themselves due to the characteristic magnetic properties of the Co and Fe impurities. We are convinced of this by a comparison with the systems considered earlier (**CrAl**, **CrSi**, **CrGe**, etc.), which have no moments but nevertheless exhibit similar anomalies. The characteristics of the magnetic impurities are manifested in anomalies in the magnetic susceptibility, electrical resistance, and, possibly, thermal expansion (the Invar effect). Unfortunately, a discussion of the results of the many experimental studies that have been done on these interesting systems in recent years is beyond the scope of this review.

4. PECULIAR TOPOLOGY OF THE FERMI SURFACE OF CHROMIUM

The transition to the excitonic insulator state and the appearance of the SDW occur only in the case of a peculiar geometry of the bands near the Fermi energy; specifically, condition (2) must be satisfied. But do such bands exist in chromium? That is, are we justified in using the excitonic insulator model to describe the properties of chromium?

The topology of the Fermi surface of the paramagnetic phase of Cr was first studied by Lomer,[12] who used the rigid-band approximation for a bcc transition metal. In other words, Lomer shifted the Fermi energy in the band structure of paramagnetic bcc iron to a level corresponding to the number of electrons in chromium. As a result he obtained a Fermi surface which agrees qualitatively with the results of later self-consistent calculations of the band structure of the paramagnetic phase.[74–77] In Fig. 10 this surface is represent-

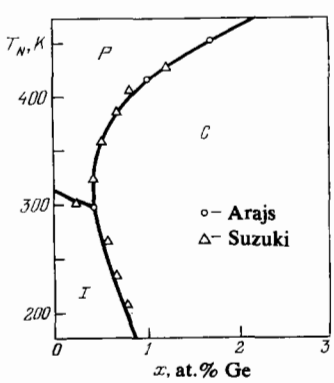

FIG. 9. Phase diagram for the alloy Cr Ge.[68,69]

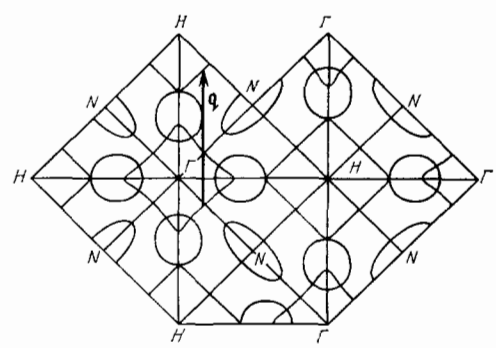

FIG. 10. Fermi surface of the paramagnetic phase of chromium, according to the calculation of Ref. 76. The arrow shows the wave vector $\mathbf{q} = \tilde{\mathbf{Q}}$ which nests the electron and hole portions.

ed in cross-sectional form by a plane passing through the center of the Brillouin zone. It has two nested portions, viz., a hole octahedron centered at the H point of the Brillouin zone, and an electron quasioctahedron centered at the Γ point. The octahedral faces are perpendicular to the (111) direction, and the electron octahedron is smaller than the hole octahedron.

A large portion of these two sheets of the Fermi surface can be nested through translation by a vector $\tilde{\mathbf{Q}} = (2\pi/a)(1-\tilde{\delta}, 0, 0)$. Then the total volumes of the electron and hole portions become approximately equal, and in the antiferromagnetic phase these portions vanish, being covered by a gap in the spectrum. The ellipsoids centered at the N point of the Brillouin zone and the spheres on the Δ lines (in Fig. 10 the cross section of these spheres is centered approximately midway between the Γ and H points) are superposed on each other in the reduced Brillouin zone and in the incommensurate phase form chain-link sheets of Fermi surface (this is shown in Fig. 11 for the hole ellipsoids). To construct the Fermi surface in the antiferromagnetic phase, because $\tilde{\mathbf{Q}}$ is incommensurate with the reciprocal lattice vector it is necessary to perform translations by vectors $\pm n\tilde{\mathbf{Q}}$ ($n = 1, 2, 3, \ldots$). The presence of chains of ellipsoids and spheres is a peculiar feature of the Fermi surface of chromium in the antiferromagnetic phase. (It is these portions of the Fermi surface, which are not covered by the insulator gap, that form the "reservoir" in the terminology of the excitonic insulator model).

The above model of the Fermi surface of chromium was first considered[78] for interpreting the frequency spectrum of the de Haas–van Alphen (dHvA) effect, and has subsequently been used by many investigators.[79–82] The main types of extremal cross sections for the chains of hole ellipsoids are shown in Fig. 11. The chains of orbitals consisting of cross sections of spheres have not been observed experimentally in view of the large effective masses associated with this portion of the Fermi surface. Data on the dHvA spectrum can be used to calculate δ and $\mathbf{Q}$.

The value of δ obtained in Refs. 80 and 81 ($\delta = 0.49$) is in good agreement with the value determined by neutron-

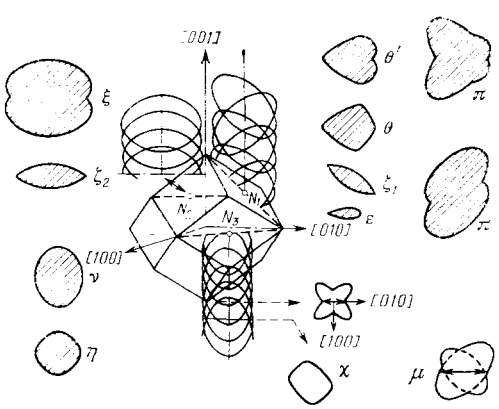

FIG. 11. Some extremal cross sections, associated with the hole ellipsoids at the N point of the Brillouin zone, for chain-link sheets of the Fermi surface.

diffraction measurements.[24] We stress that here we are talking about the same quantity δ, i.e., a measure of the deviation of the wave vector from $\mathbf{G}/2$ for the SDW itself, and not a measure of the noncoincidence of the electron and hole octahedra.

One must also note the following. All these orbitals are magnetic-breakdown orbitals, because when the ellipsoids are superposed on one another an energy gap arises at the points of intersection. This problem was first considered by Falikov and Zuckerman,[83] who used a perturbation theory in the potential causing the SDW and a simple model of the spectrum (free electrons and strongly coupled S-electrons) to obtain the values of the magnetic-field strength at which the magnetic breakdown occurs:

$$H_n \approx \frac{\hbar c}{e}\,\frac{\Delta_n^2}{8E_{\rm SS}^2(111)\,a^2} \quad \text{or} \quad \frac{mc}{e\hbar}\,\frac{\Delta_n^2}{\varepsilon_{\rm F}}\,; \tag{24}$$

here $E_{\rm SS}(111)$ is the overlap integral of the S functions of the nearest neighbors in the bcc lattice, Δ_n is the width of the energy gap arising in the nth order of overlap. In perturbation theory this quantity falls off a the nth power.

The fields H_n can be measured by observing the electronic interference, which leads to periodic oscillations of the transverse magnetoresistance for a current perpendicular to the open orbitals arising as a result of the magnetic breakdown. Arko and coworkers[84] demonstrated the existence of such orbitals in chromium and observed oscillations of the magnetoresistance. Recently these oscillations were again measured[85] and it was shown that their frequency corresponds to the area J formed by a chain of N ellipsoids. It should be stressed that J is the interference area and not the area of the orbitals in the dHvA sense, since the contributions to this area from different segments of the overlapping N ellipsoids effectively cancel. Measurement of the amplitudes of the interference oscillations yields an estimate of H_n and, accordingly, of Δ_n. For example, H_1 turns out to be 5–10 T ($\Delta_1 = 0.05$–0.07 eV), $H_2 = 0.5$–1.5 T ($\Delta_2 = 0.015$–0.27 eV), but H_3 is found to have the unexpectedly large value of 10 T.[85]

The chain-link model of the Fermi surface makes it possible to evaluate the change in $\mathbf{Q}$ under pressure. In Ref. 80 the results of measurements of the dHvA effect under pressure were used to obtain an estimate of the pressure derivative $d\ln Q'/dP = (-0.45 - 0.47)\cdot 10^{-3}$ kbar^{-1} ($Q' = Q\cdot a/2\pi$). This result is in good agreement with the neutron-diffraction results ($-0.5\cdot 10^{-3}$).[86] The chain-link model also yields the change in $\mathbf{Q}$ due to an impurity from the results of dHvA measurements. For the alloys CrMn and CrV it was estimated[87] that $d\ln Q'/dx \approx 0.022$ per atomic percent impurity, a value in good agreement with the neutron-diffraction data (0.02).[88] This confirms the applicability of the rigid-band model for these alloys.

Measurements[79] of the dHvA effect under conditions of uniaxial strain (magnetostriction oscillations) show that when rescaled for hydrostatic compression the derivative $d\ln Q'/dP$ is almost zero. Therefore, Venema and coworkers[82] made a more detailed study of the effect of pressure on the dHvA frequency and calculated the pressure derivatives

of Q. The results supported those of Ref. 80 but cast doubt on the results of Ref. 79. The contradiction was resolved in an unexpected and very interesting way. In Ref. 89 measurements were made of the dHvA effect under low pressures (up to 140 bar), at which it is possible to change the pressure continuously without heating the chamber. It was shown that the dHvA frequencies are shifted under pressure by an amount corresponding to $d \ln Q'/dP = -0.55 \cdot 10^{-3}$ kbar^{-1}, in good agreement with the data obtained in the high-pressure[80,82] and neutron-diffraction experiments, but the shift was irreversible. In other words, after the pressure is removed the vector Q does not return to its original value but remains the same as it was under pressure. If pressure is reapplied, Q does not change at first, but after the pressure has exceeded its maximum value in the first cycle one observes a further irreversible change in Q, at the same rate as at the start of the experiment. If, after the pressure is relieved, the temperature is reduced to 50–200 K, the sample is "annealed" and the vector Q returns to its original value, i.e., to the value it had in the initial unstrained state. Thus an effect is observed which is completely analogous to ordinary metallurgical quenching.

These measurements explain why the pressure derivative of Q is found to be zero in the magnetostriction measurements,[79] where the sample was continually cycled, i.e., where the stress oscillated from zero to its maximum value many times during the measurement of the shift of the dHvA-effect frequencies.

Comparison of the results of band calculations and the dHvA experiments shows that despite the good quantitative agreement between the measured and calculated[75,76] value of Q, the pressure derivative $d \ln Q'/dP$ obtained in the corresponding band-structure calculations is completely at odds with the experimental value. For example, the calculated values of $d \ln \tilde{Q}'/dP$ are $-0.1 \cdot 10^{-3}$ kbar^{-1} (Ref. 76), $+0.05 \cdot 10^{-3}$ kbar^{-1} (Ref. 90), and $+0.2 \cdot 10^{-3}$ kbar^{-1} (Ref. 91). All these values are considerably smaller in magnitude than the experimental value, and in the last two cases[90,91] have a different sign. We stress once again that both the dHvA measurements and the neutron-diffraction experiment measure the vector Q, while the band calculation gives the vector $\tilde{Q}$, i.e., a characteristic of the paramagnetic Fermi surface. The pressure dependence of $\tilde{Q}$ should be compared with the experimental results for the dHvA effect in Mo,[92] where the value $d \ln Q'/dP$ is estimated as $+0.07 \cdot 10^{-3}$ kbar^{-1}, or in W,[93] where it is $+0.1 \cdot 10^{-3}$ kbar^{-1}.

Fenton[94] has shown that in the excitonic insulator model the vector Q can change with pressure and temperature even when the vector $\tilde{Q}$ does not. Suppose that $\tilde{Q}$ does not coincide with G/2; then the optimum value of the wave vector of the SDW is determined by the extremum of the equation for the Néel temperature with respect to $\delta(q_0)$ [see Eq. (25) in Sec. 5]. The results of a numerical calculation of $\delta/\tilde{\delta}$ as a function of $\mu_0/\pi k_B T_N$ are shown in Fig. 12. Since band-structure calculations show that $\tilde{\delta}$ is a slow function of pressure while μ_0 is a rapid function of pressure, δ changes rapidly in the relevant interval of the argument $\mu_0/\pi k_B T_N$.

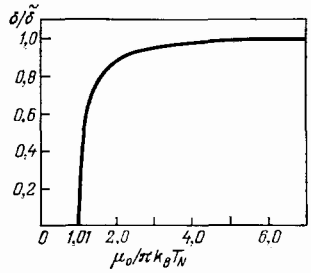

FIG. 12. Ratio of the value of δ for the SDW wave vector to the geometric value $\tilde{\delta}$ as a function of μ_0 (calculation of Ref. 95).

5. INCOMMENSURATE SPIN-DENSITY-WAVE STRUCTURE IN CHROMIUM AND ITS ALLOYS

In pure chromium the nesting discrepancy μ_0 is greater than μ_0^* (see Fig. 1), and therefore for further analysis we must generalize the excitonic insulator theory to the case of incommensurate structures. This is the subject of the present Section.

In Rice's model[22] the electron and hole Fermi surfaces are spheres of different radius, and therefore this model is degenerate with respect to the direction of the vector $\mathbf{q} = \mathbf{Q} - (\mathbf{G}/2)$. If it is assumed that the transition to the I phase is second order, the Néel temperature $T_N(\mu_0, \mathbf{q})$ can be found for structures with different wave vectors $|\mathbf{q}|$ by generalizing the gap equation (16); one should then find the value q_0 at which the temperature T_N is maximum. We ultimately get the system of equations

$$-\ln \frac{T_N}{\mathring{T}_N} = \mathrm{Re}\, \frac{1}{2} \int_{-1}^{1} \left[\Psi\left(\frac{1}{2} + i\, \frac{\mu_0 + v_F q z}{2\pi k_B T_N}\right) - \Psi\left(\frac{1}{2}\right) \right] dz,$$

$$\frac{\partial T_N(\mu_0, q)}{\partial q} = 0. \qquad (25)$$

The line $T_N(\mu_0)$ of the second-order transition to the I phase is shown in Fig. 1. It begins at the point (μ_0^*, T_N^*), at which $q_0 \to 0$, and ends on the abscissa at the point $\mu_0^c = 0.755\,\Delta_0$, $T_N = 0$. The result does not depend on the reservoir capacity β. However, attempts at a further study of the transition from the P to the I phase in Rice's model have encountered a number of difficulties.

It has been shown[95] that for $\mu = \mu_0 = \text{const}$, i.e., at an infinite reservoir capacity, the transition is first order, not second order. But in this case the line of transitions from the P phase to the I phase can be found only by a variational method, since the exact solution for the SDW structure in Rice's model is not known. Near the Lifshitz point (μ_0^*, T_N^*), where the first-order character of the P-I transition is very weakly expressed and the Ginzburg-Landau expansion can be used, the thermodynamic potential Ω has been calculated[95] for two types of SDW structures—a sinusoidal linearly polarized structure and a helical structure. It was found that the sinusoidal structure is favored in the validity region of the expansion.

The calculation in Ref. 95 shows that as one moves away from the Lifshitz point (μ_0^*, T_N^*) toward greater values of μ_0, there is a sharp increase in the parameter $v_F q_0/k_B T_N$ which characterizes the validity of the Ginzburg-Landau expansion. Consequently, in the case of a second-order transi-

tion the higher harmonics of the SDW (the Fourier components of the magnetization with wave vectors which are multiples of q_0) become more important, and one cannot say anything about the true transition line $T_N(\mu_0)$ or the true SDW structure. Strictly speaking, the same problem arises as in the case of superconductors in an exchange field (the Larkin-Ovchinnikov-Fulde-Ferell state[96,97]), where the line of transitions to the I phase cannot be found either.

The case of a fixed number of particles ($\beta = 0$) has also been considered.[98] Here the transition is actually second order. It was shown that of the two variational solutions (the sinusoidal and helical), the first is favored everywhere below T_N. In the case of an arbitrary reservoir capacity β one can obtain the conditions under which the order of the transition changes (from second to first), but we shall not go into the details of this problem since in the case of Cr the exact value of the reservoir capacity has not been conclusively established.

We also note that because of the variational character of the calculations, the fact that the sinusoidal solution is favored over the helical solution still does not guarantee that it is absolutely favored. More complicated SDW structures can be proposed, and there is no basis for excluding them from the analysis. In fact, a more complete variational analysis of the incommensurate SDW has recently been carried out[20] for structures which do not contain high harmonics. The variational procedure for finding the most favorable magnetic structure is as follows. Starting from the model Hamiltonian (7), one evaluates the Gibbs potential

$$\Omega_{\text{eff}} = \langle H_{\text{eff}} - \mu N \rangle_{\text{eff}} - TS_{\text{eff}}, \tag{26}$$

where the averaging is over the ground state of Hamiltonian H_{eff}. The set of vectors $\mathbf{q}$ is specified in such a way as to satisfy the symmetry requirements of the high-temperature phase. Specifically, for a model with a single wave vector of length $|\mathbf{q}|$ one can construct a star of vectors, $\pm\mathbf{q}_1$, $\pm\mathbf{q}_2$, $\pm\mathbf{q}_3$, directed along the axes (100), (010), and (001), respectively. For such a choice of star $\{\mathbf{q}_i\}$ the Fourier components $M_{\mathbf{q}}$ of the vectors transform according to the space group $Im\,3m$ of the cubic bcc lattice of chromium. There are 18 real parameters $\{M_{\mathbf{q}}\}$ in all.

The expansion of the thermodynamic potential Ω in invariant combinations of vectors $\{M_{\mathbf{q}}\}$ easily written down purely on considerations of symmetry.[20] The coefficients of these combinations can be evaluated from the specific microscopic model. It was shown in Ref. 20 that a configuration which is favored over the sinusoidal and helical magnetic configurations is one having three vectors $\mathbf{q}_i$ of equal modulus: $\{M_{\mathbf{q}} = \{M^x_{\pm q_1}, M^x_{\pm q_2}, M^x_{\pm q_3}\}$, i.e., the magnetization is of the form

$$\mathbf{M}(\mathbf{r}) = \mathbf{x}M_0\,[\cos(qx + \varphi_x) + \cos(qy + \varphi_y) + \cos(qz + \varphi_z)], \tag{27}$$

where $\varphi_{x,y,z}$ are constant phases which do not depend on the coordinates. We thus see that Rice's model in the above variational approach does not describe the real SDW in chromium, which has a one-dimensional SDW with a single vector $\mathbf{q}$.[2)] We stress, however, that the question of which particular SDW structure is favored cannot be finally resolved without taking the higher harmonics into account, and it is practically impossible to do this in Rice's model.

Another model of an incommensurate SDW (the octahedral model) was proposed by Kotani and coworkers.[99,100] In this model the Fermi surface of the electrons and holes are modeled by octahedra of different volumes; the octahedra have pairs of plane-parallel faces. This model is obviously close to the actual shape of the Fermi surface as discussed in the previous Section.

Considering each pair of parallel faces independently, one can assume that the Fermi-velocity vector is strictly perpendicular to the surface of the face, i.e., the problem reduces to one-dimensional. It must be noted, however, that at small values of Δ_t and $v_F q$, an arbitrary slight transverse ripple η will become important ($\Delta \lesssim |\eta|$), and this is a natural criterion for the applicability of the octahedral model for describing the SDW in chromium, which has a thoroughly finite rippling of the Fermi surface (see Fig. 10). The phase diagram of this model is calculated in Ref. 101 by the same method as was used for Rice's model.

The transition from the P phase to the C phase, as in Rice's model, is second order; the transition between the P and I phases is also second order at any reservoir capacity β, but the P-I transition line $T_N(\mu_0)$ is entirely different. It begins at the Lifshitz point (μ_0^*, T_N^*) and falls off smoothly, asymptotically approaching zero, and the transition is possible in a formal sense at any value of μ_0 (line 2 in Fig. 1).

One can do a variational calculation for magnetic structures with wave vector $\mathbf{q}$ in the octahedral model as well. It was shown in Refs. 13 and 94 that the sinusoidal solution $\mathbf{M}(\mathbf{r}) = \mathbf{x}M_0 \cos(\mathbf{q}\cdot\mathbf{r})$, where the vector $\mathbf{q}$ is directed along one of the (100) axes, is the most favorable in the class of magnetic structures considered. This is an important indication that the octahedral model gives a good description in the case of chromium.

The octahedral model also bears a strong mathematical resemblance to the so-called continuum model of Peierls, which is widely used to describe the CDW transition in quasi-one-dimensional systems. This generality, as will become clear, enables one to construct the exact SDW ground state, which is of the form of a soliton lattice, and to obtain the correct phase diagram, at least for the case of a fixed chemical potential.

Scattering by impurities and phonons was incorporated in the octahedral model in Ref. 102. The method used was analogous to that described in Sec. 2 for he spherical model. The phase diagram from Ref. 102 gives a rather good description of all the qualitative features of the actual phase diagram of alloys of Cr with nonmagnetic d-metals. According to Ref. 102, the phonons play the major role in scattering in dilute alloys of chromium. The best agreement with exper-

[2)]A real crystal can contain domains within which the vector $\mathbf{q}$ is directed along one of the three crystallographically equivalent direcions (100), (010), (001). The application of a weak external magnetic field can create a preferred orientation of the SDW vector along one of these directions (cooling in an external field). In the antiferromagnetic state this orientation persists after the field is removed.

iment for pure Cr is achieved at $\tau_{ph}^{-1} = 0.24\,\pi k_B T_N$. In this case $\mu_0^{Cr} = 0{,}55\ \Delta_0$, $T_N = 312\ K = 0.321\ \mathring{T}_N$, where $\Delta_0 = 0.15$ eV, $\mathring{T}_N = 972$ K. With these parameters the coordinates of the Lifshitz point are $(\mu_0^*, T_N^*) = (0.504\Delta_0, 0.38\ (\mathring{T}_N)$.

It should be mentioned that there is one "hidden reef" on the way to constructing the correct magnetic structure below $T_N(\mu_0)$. The appearance of an incommensurate SDW is accompanied by a modulation of the charge density. The Coulomb forces which thus arise tend to restore electrical neutrality over the scale of the long-period structure. Allowance for the direct Coulomb interaction strongly alters the coefficients of the higher terms in the Landau expansion of the free energy.

According to Ref. 103, near the line of transitions to the antiferromagnetic phase we have

$$F = 2N(0)\int f(r)\,dr, \tag{28}$$

$$f(r) = \alpha_t\Delta_t^2 + \frac{1}{2}\beta_t\Delta_t^4 + \frac{1}{3}\gamma_t\Delta_t^6 + a_1(\mathrm{grad}\,\Delta_t)^2 + a_2(\mathrm{div}\,\mathrm{grad}\,\Delta_t)^2 + b_1\Delta_t^2(\mathrm{grad}\,\Delta_t)^2. \tag{29}$$

The coefficients in (19) are written out explicitly in Ref. 103. If $a_1 < 0$, as is the case for $\mu_0 > \mu_0^*$, then the equilibrium order parameter $\Delta_t(\mathbf{r})$ becomes inhomogeneous (this corresponds to a transition to the I phase of the SDW. This causes a redistribution of the electron density $n(\mathbf{r})$, giving rise to a slowly varying potential $\varphi(\mathbf{r})$ in the system:

$$\varphi(\mathbf{r}) = \int \frac{e^2}{|\mathbf{r}-\mathbf{r}'|}[n(\mathbf{r}') - n]\,d\mathbf{r}', \tag{30}$$

where $n = \langle n(\mathbf{r})\rangle$ is the average value of the electron density

$$n(\mathbf{r}) = T\sum_{\omega_n} \mathrm{Sp}\,\hat{G}_{ll}(\omega_n) + N_r(\mu - \mu_0 + \varphi(\mathbf{r})), \tag{31}$$

and N_r is the density of states in the reservoir.

It is in principle important to take the long-range part of the potential $\varphi(\mathbf{r})$ into account [Eq. (30) is simply Poisson's equation]. If one formally sets $e^2 = 0$, the Landau expansion of the free energy F acquires nonlocal terms of the type $\langle\Delta^2(\mathbf{r})\rangle^2$ (here $\langle\ldots\rangle$ denotes a volume average). Because of the Coulomb character of the interaction $\varphi(\mathbf{r})$, even at arbitrarily small nonzero values of e^2 the nonlocal contributions completely vanish, giving way to local expressions of the type $\langle\Delta^4(\mathbf{r})\rangle$.

Similar nonlocal contributions also arise in the one-dimensional octahedral model. One can show that in this case correct allowance for the Coulomb interaction restores the local nature of the functional.[104]

Below the temperature $T_N(\mu_0)$ an incommensurate transverse structure with a SDW contains a number of subtle and interesting effects. One of these is the appearance of a strain wave, which was detected experimentally by Tsunoda *et al.*[105] using x-ray diffraction and later by Eagen and Werner[106] using neutron diffraction. The third harmonic of the SDW was obtained by Pynn *et al.*[107] using neutron diffraction. At the same time the second harmonic of the SDW has not been observed in spite of careful search. The amplitude σ of the strain wave in the alloys CrMn and CrV is proportional to the square of the amplitude of the first harmonic of the SDW,[108] just as in pure Cr.

A careful study of the higher harmonics of the spin-density and strain waves has recently been carried out[109] for Cr and its alloys with Mn and V by the neutron-diffraction method. The amplitude of the third harmonic Δ_{3Q} of the SDW is extremely small [with a ratio $\Delta_{3Q}/\Delta_t \approx (1.3-1.6)\cdot 10^{-2}$], and the higher harmonics have not been observed in neutron-diffraction experiments; this apparently indicates that they are extremely weak. The displacement $\boldsymbol{\sigma}$ of the atoms relative to their position in the ideal lattice of the paramagnetic phase, $\Delta\mathbf{R}_j = \mathbf{R}_j - \mathring{\mathbf{R}}_j = \boldsymbol{\sigma}\sin(2\mathbf{Q}\cdot\mathring{\mathbf{R}})$, where the vector $\boldsymbol{\sigma}$ is parallel to $\mathbf{Q}$, amounts to $(0.89 \pm -0.16)\cdot 10^{-3}\,a$. The third harmonic grows with increasing Mn concentration and falls off with increasing V concentration (but in the commensurate SDW phase of CrMn the higher harmonics are absent altogether). The amplitude of the strain wave varies extremely slowly in the alloys CrMn and CrV in comparison with pure chromium. The higher harmonics of the strain wave have not been detected either. Figure 13 shows a schematic illustration of the model for two possible phase relationships between the first and third harmonics of the SDW.[110] It should be noted that everywhere here we are discussing the region above the spin-flip transition.

As we have mentioned, in the excitonic insulator model, in addition to the anomalous averages Δ_t which describe a SDW (the triplet order parameter), there are also anomalous averages which describe a charge-density wave.[111] One can easily see from the Hamiltonian (2) that the appearance of an incommensurate SDW with wave vector $\mathbf{Q} = (\mathbf{G}/2) \pm \mathbf{q}$ automatically gives rise to a CDW with $\mathbf{q}_1 = \pm 2\mathbf{q}$. The component with $\mathbf{q}_1 = \pm 2\mathbf{q}$, which is proportional to $\Delta_{t,\pm\mathbf{q}}\Delta^*_{t,\pm\mathbf{q}}$, leads to a period-doubled (in comparison with the SDW) modulation of the electron density. The presence of an electron-phonon interaction gives rise to a periodic strain with wave vector $2\mathbf{q}$.

All these arguments are valid if the problem is solved in perturbation theory and the terms of lowest order in the SDW amplitude are kept. Generally speaking, the higher harmonics that can arise are the even harmonics of the charge-density and strain waves with wave vectors $2n\mathbf{q}$ and the odd harmonics of the SDW with wave vector $(2n+1)\mathbf{q}$.

If $\Delta_t \sim T, \mu_0$ there are no grounds for assuming that the

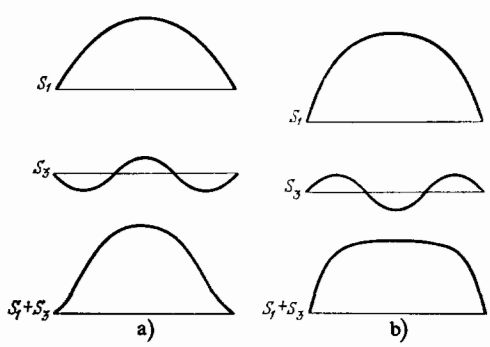

FIG. 13. Possible phase relationships (*a* and *b*) between the first (S_1) and third (S_3) harmonics of the SDW.[110]

amplitudes of the higher harmonics of the SDW and CDW are small compared to Δ_r. The electron spectrum of chromium below T_N should therefore contain a set of microgaps, which should be manifested in the optical absorption. Actually, however, no series of peaks has been detected in optical experiments. We shall return to this question shortly.

The higher harmonics of the spin-density, charge-density, and strain waves have been taken into account in a systematic manner in a series of papers by Kotani.[101,112] All the experimental results are reproduced fairly well in the numerical calculations,[112] but on the basis of this fact alone it is difficult to say with certainty that the octahedral model can be used for quantitative description of the SDW in chromium. The introduction of many complications (spin polarization of the reservoir electrons in the field of the SDW, imperfect nesting, interactions with phonons) essentially vitiates the original advantages of the octahedral model, viz., its one-dimensionality and the possibility of obtaining analytical results.

However, the description of incommensurate structures by the usual methods of band theory is practically impossible, and therefore the octahedral model with complicating modifications is an intermediate link between numerical calculations from first principles and an analytical theory.

It must be said, however, that the question of the order of the phase transition between the C phase and I phase essentially remains unresolved in the models we have discussed. The reason for this is that as one approaches the line of this transition a larger and larger number of harmonics come into play; in other words, the number of relevant harmonics increases without bound. Nevertheless, Buzdin and Tugushev[113] recently succeeded in obtaining the exact phase diagram of the octahedral model and constructed the exact line of the C-I phase transition. They did this using the exact solution of the one-dimensional Peierls model, as obtained by Brazovskiĭ and coauthors[114] and by Horovitz.[115] The exact solution for the triplet order parameter has the form of a soliton lattice:

$$\Delta_t(x) = \mathring{\Delta}_t \operatorname{sn}\left(\frac{x\mathring{\Delta}_t}{v_F\gamma}, \gamma\right), \tag{32}$$

where $\operatorname{sn}\zeta$ is the Jacobi elliptic function and the parameter γ takes on values $0<\gamma<1$. The quantities $\mathring{\Delta}_t$ and γ are functions of temperature and the chemical potential μ_0. In the case of a fixed chemical potential the C-I transition is first order, while in the case of a fixed number of particles it is second order. Thus the octahedral model is completely integrable at any temperatures. On the P-I transition line the parameters γ and $\mathring{\Delta}_t$ go to zero in such a way that solution (32) goes over to a purely sinusoidal solution with wave vector $\mathbf{q}_0 = \mathring{\Delta}_t/v_F\gamma = \text{const}$.

On the I-C transition line at fixed μ_0 the commensurate structure arises discontinuously at any temperatures except at the isolated point $T=0$ ($\tilde{\mu}_0 = 2\Delta_0/\pi$ and $T = T_N^*$, where the transition is second order. In a recent paper[116] Kotani also obtained the I-C transition line (or more precisely, the line of absolute instability of the commensurate phase, since it was assumed that the transition is second order) for the

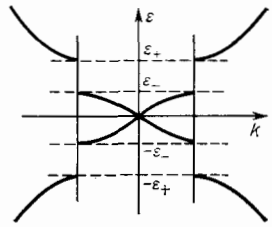

FIG. 14. One-electron spectrum in the soliton-lattice model.[114]

spin-Peierls transition in the XY model in a magnetic field. From a mathematical standpoint this system is completely identical to the octahedral model with fixed μ_0. The results of analytical[113] and numerical calculations have turned out very similar. The corresponding line $T_{IC}(\mu_0)$ is given in Fig. 1.

We also note that analysis of the neutron-diffraction data on the strain-wave and SDW amplitudes in Cr and in the alloys CrMn and CrV has led [117] completely independently to the empirical conclusion that the relationships of the amplitudes and wave vectors are best satisfied when the spatial dependence of the magnetization is of the form (32), i.e., a soliton lattice.

The spectrum of the soliton structure has only two gaps (Fig. 14) and a narrow allowed band which vanishes at the transition to the commensurate structure. Curiously, all the optical absorption measurements in the I phase have revealed only two peaks,[118] which have been interpreted in a rather artificial way.[26] It is clear that in the case of the soliton lattice the frequencies of these peaks are $2\varepsilon_+$ and $(\varepsilon_+ - \varepsilon_-)$; here

$$\varepsilon_\pm = \frac{\Delta_t}{2}\left(\frac{1}{\gamma} \pm 1\right).$$

In pure chromium the frequencies of the absorption peaks are 0.15 and 0.45 eV, giving $\gamma \approx 1/2$. In CrMn there is only one absorption peak, at ~ 0.4 eV; this circumstance can be interpreted as the vanishing of the narrow soliton band at the I-C transition, where $\gamma \to 1$, $\varepsilon \to 0$.

Let us now return to the effects of an interaction between the incommensurate SDW and the crystal lattice, considering the phenomenological description of this interaction in more detail.

Because there is no linear coupling between the triplet order parameter Δ_t and the strain tensor η_{ij}, the lattice distortion will be only of order Δ_t^2. A temperatures close to T_N one can use the Ginzburg-Landau functional. In a recent paper[119] Walker constructed a two-parameter Ginzburg-Landau functional with allowance for the spatial symmetry of the bcc cell of chromium. No specific model of the chromium band structure was used in that paper, and the coefficients in the free energy were treated simply as phenomenological parameters. When the elastic properties of the lattice are taken into account, the transition to the I phase of the SDW turns out to be first order, but close to second order, and at the Néel point there is a discontinuity in the elastic modulus C_{11} [along the (100) direction]. The transition to the SDW state under pressure was investigated by this same scheme.[119,120]

At temperatures $T < T_N$ the situation is considerably more complex, and we do not yet have a consistent theory of an incommensurate SDW interacting with the lattice. This problem is extremely interesting, however, particularly in regard to the aforementioned quenching of the wave vector of the SDW[89] (see Sec. 4). Fenton[121] attempted to explain this effect by analogy with the Back-Timonen[42] model for the incommensurate charge-density wave, using the results of Ref. 122.

The Back-Timonen model, which is based on an idea due to McMillan,[41] describes a system in which the CDW is coupled to the lattice through the interaction of fluctuations in the phase of the CDW with fluctuations in the phase of the lattice with respect to the stable positions in the commensurate structure. In the phase-soliton (CDW domain-wall) region, lattice domain walls (dislocations) form. The energy of these dislocations is negative, and with increasing pressure they multiply on account of the increasingly incommensurate structure. At low temperature the excess lattice dislocations do not have time to be "reabsorbed" after the pressure is removed, and for practical purposes the SDW is pinned at these dislocations. The system thus remains in a metastable state, and an annealing is needed in order to return it to a truly equilibrium state.

An alternative explanation for the quenching of the wave vector of the SDW (by analogy with the CDW) was proposed by Littlewood and Rice.[123] They attributed this effect to the pinning of phase solitons (excited metastable states of the SDW) at random defects. They believed[123] that it was just such metastable states of the SDW that were observed in the low-temperature experiments.[89] A Monte Carlo calculation for the case of a one-dimensional CDW in the chain model with 200 randomly distributed impurities (the average distance between impurities was taken to be 100 wavelengths of the SDW) did in fact reveal the presence of hysteresis in the $\mathbf{q}$ dependence of $\langle \nabla\varphi \rangle$ [here $\mathbf{q}$ is the change in the wave vector of the lattice, simulating the effect of pressure, $\langle \nabla\varphi \rangle$ is the average gradient of the CDW phase, $\Delta_s(x) = \Delta_0 \cos(Qx + \varphi(x))$, and $\mathbf{Q}$ is the wave vector of the CDW in the ground state (at zero pressure)]. With increasing $\mathbf{q}$ the value of $\langle \nabla\varphi \rangle$ grows with a certain slope, and with decreasing $\mathbf{q}$ it falls off with a different slope. The presence of hysteresis indicates that the excited states of the CDW (and SDW) are separated from the ground state by an energy barrier, and after a rapid removal of the external influence the system is unable to return to the ground state.

6. GROUND-STATE PROPERTIES AND MAGNETIC EXCITATIONS IN CHROMIUM

The direct connection between the topology of the Fermi surface and the antiferromagnetic ordering in chromium has stimulated a large number of calculations of the band structure of this metal in the paramagnetic state. Calculation of the antiferromagnetic phase, however, is a practically unsolvable problem since it is impossible to calculate the incommensurate SDW structure in the ordinary band approach. Therefore, it is important to estimate the degree of applicability of the excitonic insulator model for describing the commensurate case by making direct calculations of the ground-state energy and other characteristics; the corresponding band calculations will provide the necessary numerical parameters which, if the program is successful, might be used in the excitonic insulator model to describe the incommensurate phase.

Calculations of the commensurate antiferromagnetic phase of Cr, which has a magnetic structure of the CsCl type, have recently been done using three different methods of evaluating the one-electron spectrum,[90,91,125] with different approximations for the effective exchange-correlation interaction (in the density-functional formalism). It must be stressed that the density-functional formalism in principle guarantees the correctness of the description of the properties of the ground state (but not quasiparticle states) in terms of the solution of the single-particle problem if the form of the exchange-correlation potential is known.

Calculations[90,91,125] using this method have yielded the value of the spontaneous magnetization: $0.59\,\mu_B$ at a lattice constant $a = 5.483$ a.u.,[91] $0.48\,\mu_B$ at $a = 5.442$ a.u.,[90] and $0.29\,\mu_B$ at $a = 5.397$ a.u.[125] (the experimental value is 0.59 μ_B at $a = 5.397$ a.u.). The binding energy comes out rather well (4.61 eV,[91] compared with an experimental value of 4.09 eV), as does the modulus of hydrostatic compression (1.62 Mbar[91] and 2.36 Mbar,[125] compared with an experimental value of 1.9–2.1 Mbar).

We believe that one of the most important results from these calculations is Kübler's evaluation[91] of the difference $\Delta E = E_{AFM} - E_{PM}$ between the total energies of the antiferromagnetic and paramagnetic states; this difference is written as a sum of five terms:

$$\Delta E = \Delta E_{ion} + \Delta E_{val} + \Delta E_x + \Delta E^{xc}_{pot} + \Delta E_{xc}, \qquad (33)$$

where the first and second terms are the sums of the one-electron energies for the ionic-core and valence electrons, respectively, the third and fourth terms are due to the double counting of the direct Coulomb and exchange-correlation interactions, and the last term is the difference between the exchange-correlation energies. The first four terms in (33) give a value $+0.06$ eV, i.e., a disadvantage in total energy upon formation of the antiferromagnetic state, but $\Delta E_{xc} = -0.12$ eV, and so the antiferromagnetic state is stable. The system of valence electrons has an energy advantage, equal to -0.03 eV, that is completely outstripped by the large values of the other four contributions. However, these contributions compensate one another, and the net value $\Delta E = -0.06$ eV is close to the contribution from the valence electrons. In Ref. 90 the parameters obtained in the band calculation [g, N(0), μ, Δ] were used to estimate the energy advantage for the valence electrons with the aid of the formula from the excitonic insulator model. The result, -0.02 eV, agrees satisfactorily with the results of direct numerical calculations.

All the band calculations give a value for the antiferromagnetic gap that is larger than the value obtained from an elementary excitonic-insulator model of the BCS type. In particular, values of 0.51 and 0.48 were obtained for the commensurate phase in Refs. 90 and 91, respectively. These values are in reasonable agreement with the experimental

values of the gaps[118] in commensurate CrMn and CrRe alloys (0.36–0.40 eV). The somewhat smaller experimental value of the gap is easily explained by the additional influence of impurity scattering, which was not taken into account in the band calculations of the commensurate phase. In addition, it can be shown[126] that an excitonic insulator model incorporating impurity scattering, in which case the parameter τ^{-1} in (21) is of the form $\tau^{-1} = \Gamma_0 + \alpha T$, $\Gamma_0 = 7.8$ meV, $\alpha = 0.13$ meV/K, can yield a value 0.3 eV, rather close to the experimental and band-calculation results. The value of the effective interaction constant $U = 0.43$ was adjusted to give $T_N = 515$ K, corresponding to the experimentally measured value for an alloy with 2% Mn. Band calculations[91,90] give a similar value for the effective constant: $U = 0.4$–0.55.

The effect of pressure on the antiferromagnetic gap and spontaneous moment is a good illustration of the need for the excitonic insulator model in order to interpret correctly the results not only of experiments but also of numerical calculations. The authors of Refs. 90 and 91 gave incorrect estimates of the pressure derivatives of the gap and moment. The error lay in the customary assumption that the properties of transition metals have a linear pressure dependence. Therefore, the numerical calculation, which levels out the exponential pressure dependence of the parameters of the ground state, gives a value which differs from the experimental by an order of magnitude. The pressure derivative of the gap satisfies the relation

$$\frac{d\ln\Delta}{dp} = \frac{d\ln\varepsilon_F}{dp} - \frac{d}{dp}\left(\frac{1}{U}\right), \quad U = gN(0), \tag{34}$$

where the effective electron-electron interaction $g = 0.547$ Ry is calculated in the density-functional formalism and has a pressure derivative $d\ln g/dp = 5\cdot 10^{-4}$ kbar^{-1}. This leads to a value $d\ln\Delta/dp = -11.5\cdot 10^{-3}$ kbar^{-1}, in satisfactory agreement with experiment ($-18\cdot 10^{-3}$). We note that the first term in (34) is negligibly small, and the negative sign of the pressure derivative is due to the decrease with pressure of the density of states for the nested portions of the Fermi surface.

Using the relation $\Delta = gM$, one can also evaluate the pressure derivative of the magnetic moment, $d\ln M/dp = -1.1\cdot 10^{-2}$ kbar^{-1}. This value is also in reasonable agreement with the experimentally measured value ($-2\cdot 10^{-2}$ kbar^{-1}).

An important measurable quantity which can be calculated both in band theory and in the excitonic insulator model is the magnetic susceptibility $\chi(q,\omega)$. The static susceptibility $\chi(q,0)$ in the limit $q\to 0$ gives the response to a uniform magnetic field, and $\chi(Q,0)$ should have a sharp peak at $q = \tilde{Q}$. The poles of the dynamic susceptibility $\chi(q,\omega)$ determine the magnon spectrum of the system.

An expression for $\chi(0,0)$ in the excitonic insulator model was first obtained by Maki and Sakurai,[124] who considered the C phase with allowance for scattering by impurities.

The temperature dependence of the static magnetic susceptibility has been considered[29,127] in the framework of Rice's model with allowance for scattering by noninteracting impurities and phonons. The most complete treatment of the problem of evaluating $\chi(q,0)$, with allowance for the imperfect superposition of the electron and hole pockets and the interaction of the SDW with the magnetic moment of the impurity, was recently given in Ref. 128.

In the directions perpendicular to the polarization direction of the SDW the magnetic susceptibility tensor is the same as in the paramagnetic case, i.e., it is of the form of the ordinary Pauli contribution $\chi_\perp = \mu_B^2 N(0) \equiv \chi_0$, but in the direction parallel to the polarization of the SDW it has the more complicated temperature dependence

$$\chi_{\parallel} = \chi_0\left(1 - \frac{2\pi}{k_B T}\,\mathrm{Re}\,\Gamma\right), \tag{35}$$

$$\Gamma = \sum_{n=0}^{\infty}\left\{1 + \frac{\tilde{\omega}_n^2}{\tilde{\Delta}_n^2}\sqrt{\tilde{\Delta}_n^2 + \tilde{\omega}_n^2}\left[1 + \frac{\Delta - \tilde{\Delta}_n}{\tilde{\Delta}_n}\,\frac{(\tilde{\omega}_n^2/\tilde{\Delta}_n^2) - 1}{(\tilde{\omega}_n/\tilde{\Delta}_n) + 1}\right]\right\}^{-1}, \tag{36}$$

where $\tilde{\omega}_n$ and $\tilde{\Delta}_n$ are solutions of the system of equations

$$\tilde{\Delta}_n = \Delta - \frac{1}{2\tau}\,\frac{\tilde{\Delta}_n}{\sqrt{\tilde{\omega}_n^2 + \tilde{\Delta}_n^2}}, \tag{37}$$

$$\tilde{\omega}_n = \omega_n + \frac{1}{2\tau}\,\frac{\tilde{\omega}_n}{\sqrt{\tilde{\omega}_n^2 + \tilde{\Delta}_n^2}}. \tag{38}$$

In expression (35) χ_0 was chosen[29] such that the theoretical value coincides with the experimental value at a certain temperature, and μ was varied to give the best fit for the temperature dependence. Above the temperature of the spin-flip transition a good agreement could be obtained[29] between the calculation and experiment (Fig. 15), but the value of the gap Δ_0 here is in poor agreement with experiment. This is not surprising, since to single out the spin-susceptibility contribution from the experimental curve is a difficult and ambiguous undertaking. The orbital (specifically, the Van Vleck) paramagnetic susceptibility was not taken into account directly in the model but was given in terms of the experimental value of the susceptibility at a certain temperature. Such a fitting to experiment should distort the other physical characteristics of the system, which were not checked during the fitting.

The problem of evaluating the total susceptibility of the paramagnetic phase from first principles was solved in Ref. 129. Calculations were done not only for the static bulk susceptibility but also for the total magnetic form factor $\chi(G)$ of the induced magnetization. The calculation of the spectrum

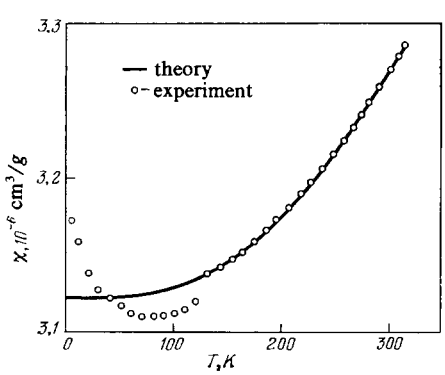

FIG. 15. Calculated[29] susceptibility χ as a function of temperature in the excitonic insulator model.

and wave functions were calculated by the linearized augmented-plane-waves method. The total theoretical form factor was obtained by combining the Van Vleck orbital, Pauli spin, and diamagnetic form factors. The calculation showed that the Van Vleck susceptibility is $130 \cdot 10^{-6}$ emu/mole, the Pauli susceptibility is $18.8 \cdot 10^{-6}$ emu/mole, and the diamagnetic susceptibility is $43.7 \cdot 10^{-6}$ emu/mole. It must be stressed, however, that the Pauli susceptibility was calculated without the exchange enhancement, which can be considerable (a factor of ~ 2.5), but this does not alter the fact that the main contribution to χ_0 is the paramagnetic Van Vleck orbital susceptibility. We note that the experimental value of $\chi(0, 0)$ for the paramagnetic phase is $140 \cdot 10^{-6}$ emu/mole and that a more exact calculation[130] gives $106 \cdot 10^{-6}$ emu/mole.

There is considerable interest in calculating the generalized static susceptibility $\chi(\mathbf{q}, 0)$ from first principles, since the presence of an anomaly in this function at $\mathbf{q} = \tilde{\mathbf{Q}}$ is an important justification for using the excitonic insulator model. Such a calculation was done for the case of Cr in Ref. 131. We note the following circumstances. First, in calculating $\chi(\mathbf{q}, 0)$ in the excitonic insulator model one usually uses only the geometry of the energy bands in the calculation; this is equivalent to using the approximation of constant matrix elements in the calculation of $\chi(\mathbf{q}, 0)$ and neglecting the effects of the local field. The value $\chi^0(\mathbf{q}, 0)$ calculated for Cr under these approximations does in fact exhibit the highest peak at $\mathbf{q} = \tilde{\mathbf{Q}}$, i.e., for the nesting vector of the octahedral electron and hole surfaces (see Fig. 10). Second, the calculations of Ref. 131 have demonstrated the necessity of simultaneously taking into account both the different probabilities for transitions between bands at different points of the Brillouin zone (a nonconstant matrix element) and the effects of the local field, i.e., the presence of Umklapp processes characterized by the reciprocal lattice vector $\mathbf{G}$. In this case criterion (1) for instability of the paramagnetic phase becomes[131] $1 = I\Sigma_{\mathbf{G}}\chi(\mathbf{q} + \mathbf{G}, \mathbf{q} + \mathbf{Q}, 0)$, i.e., the instability is determined not by the function $\chi(\mathbf{q}, 0)$ itself, but by the sum of interband susceptibilities with different reciprocal lattice vectors. Furthermore, since the function $\chi(\mathbf{q}, 0)$ has an anomaly due to the topology of the Fermi surface not only for the vector $\tilde{\mathbf{Q}} = (2\pi/a)(1 - \tilde{\delta}, 0, 0)$, but also for the vector $\tilde{\mathbf{Q}}' = (2\pi/a)(1 + \tilde{\delta}, 0, 0)$, upon summation these anomalies add. At the same time for random peaks $\chi(\mathbf{q}, 0)$ such an enhancement does not occur, and consequently, as can be seen in Fig. 16, the highest peak in fact arises at $\mathbf{q} = \tilde{\mathbf{Q}}$. We stress that the function shown in Fig. 16 is very similar to the susceptibility $\chi^0(\mathbf{q}, 0)$ of the excitonic insulator model at large values of $\mathbf{q}$. Moreover, there is even semiquantitative agreement, to within 20–25%. At small $\mathbf{q}$ the curves are qualitatively different because at $\mathbf{q} \to 0$ the matrix elements for the interband transitions also go to zero.

While numerical calculations of $\chi(\mathbf{q}, 0)$ are very time-consuming, it is an even more complicated problem to evaluate the dynamic susceptibility function $\chi(\mathbf{q}, \omega)$, even without allowance for electron-hole pairing or impurity scattering. To this day there have been no such calculations using the actual band structure, although the dynamic susceptibility

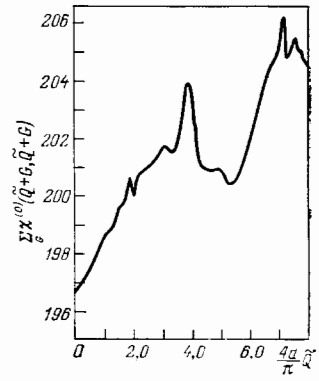

FIG. 16. The function $\Sigma_{\mathbf{G}}\chi(\tilde{\mathbf{Q}} + \mathbf{G}, \tilde{\mathbf{Q}} + \mathbf{G})$ in units of states/ Ry×atom).[131]

function has been calculated in the excitonic insulator model for systems with a SDW instability. The first such calculation of $\chi(\mathbf{q}, \omega)$ was apparently done in the random-phase approximation (RPA) by Liu,[126] who used the octahedral model for the single-particle spectrum and considered the commensurate case $\tilde{\delta} = 0$.

Liu's calculation[126] of the imaginary part of the susceptibility of chromium yielded the line shapes for magnons in the antiferromagnetic phase and for paramagnons (Fig. 17), and also for the single-particle excitations. In this regard we note that spin fluctuations or paramagnons have recently been observed in chromium at $T > T_N$.[138] A relatively slight smearing of the peak near 001 on the neutron-diffraction patterns as the temperature is raised is evidence of short-range order in chromium at $T > T_N$. The results of a calculation of the ground state of chromium in self-consistent fluctuation theory[59] indicate that there is no well-defined local magnetic moment in Cr. At the same time, experiments on diffuse neutron scattering[63] in pure chromium, like the experiments on the thermal expansion of alloys,[173] indicate that paramagnons with small wave vectors are long-lived. These effects cannot be explained in terms of the excitonic insulator model, since this model does not incorporate the effects of short-range magnetic order, and the paramagnons (see Fig. 17) are damped out much faster than in experiment.

Liu's calculation[126] also yielded the spin-wave velocity in chromium, $c = 2.5 \cdot 10^{-7}$ cm/sec, a value which is almost twice as large as the measured[133,134] value $(1.3–1.5) \cdot 10^7$ cm/sec. A similar result was also obtained in Refs. 13 and 132.

A complete derivation of the equations giving the dynamic susceptibility function in the random-phase approximation with allowance for impurity scattering and the interaction of the SDW with the magnetic moments of the impurities was recently carried out by Ami and Young.[135] Attempts have been made[136,137] to improve the agreement between theory and experiment for the spin-wave velocity by going beyond the RPA. In the "frozen magnon" method[135] an attempt is made to put the scattering by static spin fluctuations effectively on a self-consistent footing (a "frozen magnon" is simply an excitation which corresponds to static deviations of the spins from the equilibrium position). In Ref. 137 Liu used Rice's model for the electron spectrum and

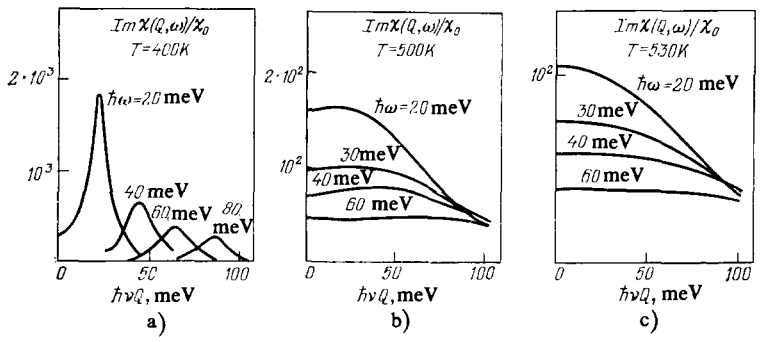

FIG. 17. Magnon line shapes below the Néel temperature (a) and close to T_N (b), and the paramagnon line shape above T_N (c). The calculations in the excitonic insulator model were done in Ref. 126.

calculated the change in energy upon a change in the orientation of the spins. The resulting value of the spin-wave velocity in chromium, $c = (1.6\text{–}1.1) \cdot 10^7$ cm/sec, is in much better agreement with experiment.

This approach effectively incorporates not only the interband spin-spin interaction but also the intraband interaction, which had not been taken into account previously. The fact that an interaction of this kind decreases the spin-wave velocity also follows immediately from Ref. 136, in which a direct calculation was made of the spin-spin interaction between the electrons of the peculiar bands and the electrons of the reservoir. The results of the two calculations[136,137] are practically the same.

7. OTHER SYSTEMS WITH SPIN-DENSITY-WAVE INSTABILITY

Until now we have been discussing mainly the properties of the SDW state in chromium and its dilute alloys. However, there are a number of indications that a similar situation also arises in certain other systems which undergo an antiferromagnetic transition.

This class of systems includes the intermetallic compound $TiBe_2$, a Laves phase with the C15 structure. In 1978, on the basis of magnetic susceptibility measurements, Matthias and coauthors[139] announced that $TiBe_2$ is the first "true" itinerant antiferromagnet, with $T_N = 10$ K. In stating this the authors had in mind that neither of the elements in the intermetallide was ever suspected of having a local magnetic moment.

However, the situation has turned out to be more complicated than was first assumed. Subsequent measurements[140,141] have definitely shown that $TiBe_2$ is a paramagnet with a strong exchange enhancement and can even become an itinerant metamagnet in a magnetic field. Moreover, the low-temperature (~ 2 K) measurements remain poorly understood. In particular, there are anomalies in the specific heat[142] and resistance[140] at this temperature.

For an explanation of these anomalies Enz[143] looked to the excitonic insulator model, whose application here is justified by the results of a calculation of the band structure[144,145] of the paramagnetic phase of this intermetallide. The calculated Fermi surface has parallel flat parts of the electron and hole types (the Γ–K direction). Moreover, estimates of the parameters of the excitonic insulator model from the experimental data and the results of band structure calculations reveal an important discrepancy between calculation and experiment: Specific-heat measurements yield the density of states of the nested portions as $N(0) = 49$ states/(Ry unit cell), but this is close to one-third of the total density of states at the Fermi energy.[3)] Enz arbitrarily took[143] $N(0) = 10$ states/(Ry unit cell).

This discrepancy between the experimental estimate of the "bare" (band) density of states and the value required for the model is most likely due to the anomalously large exchange enhancement that has been noted in this system. Replacing part of the Be atoms by Cu atoms in this alloy will give rise to ferromagnetism,[146] whereas alloying with Ga will destroy the anomalous paramagnetism.[147] To explain the properties of $TiBe_2$ it is apparently every bit as necessary to take spin fluctuations into account in the spirit of self-consistent fluctuation theory as it is to take into account the topology of the Fermi surface.

Enz's estimate[143] of the critical field H_c for destruction of the SDW state in $TiBe_2$ is extremely small: $H_c = 610$ Oe. Therefore, the results of Ref. 141, where magnetic fields above this value were used in the measurments, cannot be taken as direct evidence against the existence of antiferromagnetic ordering in $TiBe_2$.

A quite similar situation also arises in the intermetallide CrB_2, where the antiferromagnetic ordering occurs at $T_N = 85$ K.[148] It was also observed that in this compound the susceptibility is an order of magnitude larger than in other diborides (ScB_2, TiB_2, VB_2), and the electronic specific heat is also anomalously large.[149,150] This is a clear indication of anomalous exchange enhancement, i.e., of the proximity of the electronic system to the boundary of ferromagnetic instability. In addition, neutron-diffraction measurements at liquid-helium temperature reveal the existence of weak satellites which are probably of magnetic origin.

The band-structure calculation of Ref. 151 demonstrates the presence of flat parts of the Fermi surface. Liu and coauthors[151] have attempted to explain the antiferromagnetic ordering in CrB_2 on the basis of the excitonic insulator model. Their estimates are consistent with one another and give a value of the spontaneous magnetization $M = 0.01$ μ_B that agrees with the experimental value.

A general feature of the compounds considered above is the presence of susceptibility anomalies not only at $\mathbf{q} = \tilde{\mathbf{Q}}$

[3)]The transition temperature corresponding to this density of states in the excitonic insulator model would be an order of magnitude higher than the experimentally observed value.

(the anomalies responsible for the antiferromagnetic transition) but also at $\mathbf{q} = 0$. The $\mathbf{q} = 0$ anomaly, although it does not give rise to a ferromagnetic instability, nevertheless causes an anomalously large electron-paramagnon interaction. Such an interaction can clearly lower the Néel temperature by an appreciable amount.

Other interesting systems are the vanadium chalcogenides: VX, V_3X_4, V_5X_8, VX_2, X = S, Se. These phases have a metallic conductivity, and their crystal structure varies from the NiAs type to the CdI_2 type as the chalcogen concentration is increased from VX to VX_2. At the intermediate compositions they have ordered structures with completely and partially filled hexagonal layers of vanadium atoms.[152]

It is stated in a handbook[153] that there is an antiferromagnetic transition in VS at $T_N = 1040$ K, and according to Ref. 154 the magnetic susceptibility at $T > T_N$ obeys the Curie-Weiss law. No other data on the magnetic properties of VS are to be found in the literature, but it is known that the hexagonal structure of VS is unstable against small orthorhombic distortions. A band-structure calculation made in Ref. 155 showed that the Fermi surface has nested electron and hole pockets centered around the U and Δ directions. According to Liu,[156] it is these pockets that are responsible for the structural transition from the NiAs to the MnP lattice, i.e., the orthorhombic distortion is explained by the onset of a CDW in the system. The existence of an antiferromagnetic transition was ignored in this paper.

For dichalcogenides of vanadium (and niobium) the early studies also assumed the existence of an antiferromagnetic transformation, but it is now known that these substances have complex structural transitions (commensurate and incommensurate) which are not accompanied by magnetic ordering. It has not been ruled out that the transition in VS was simply identified incorrectly, and so additional neutron-diffraction and Mössbauer studies are needed.

The experimental situation is much clearer in chalcogenides of intermediate composition, which exhibit an ordering of vacancies in the partially filled vanadium layers.

V_3S_4. According to Ref. 157, the Néel temperature determined from the spin-echo spectra is 9 K and the effective magnetic moment below T_N for V atoms in vacancy layers is $0.06\mu_B$. Measurments of the magnetic susceptibility[158] have revealed a slight bend at the Néel point, and the effective moment determined from the paramagnetic susceptibility (according to the Curie-Weiss law) is $0.2\mu_B$. Both above and below T_N the conductivity is metallic.

V_3Se_4. The properties of this compound are generally analogous to those of V_3S_4,[157] but the Néel temperature is higher: $T_N = 16$ K.

V_5S_8. Magnetic-susceptibility and NMR measurements[159] in this compound give $T_N = 29$ K. The magnetic moments at the V atoms are different, i.e., they depend on the layers to which the atoms belong ($0.15\mu_B$–$0.22\mu_B$). This makes it hard to interpret the NMR data. The effective magnetic moment determined from measurements of the paramagnetic susceptibility is from 1.1 to $2.5\mu_B$ per V atom depending on whether the atom belongs to a vacancy layer or a completely filled layer. One notices a relatively strong temperature dependence $\chi(T)$ near the transition. The conductivity of V_5S_8 is metallic at all temperatures.

V_5Se_8. For this compound it has been found[160] that $T_N = 35$ K, that the temperature dependence $\chi(T)$ is rather complex, and that the relaxation rate of the nuclear spin is temperature dependent. The temperature dependences are hard to interpret in the Heisenberg model, although the material does follow the general tendency for substances of this class to exhibit an increase in $\chi(T)$ with decreasing temperature (in the paramagnetic phase). On the basis of simultaneous measurements of the NMR and magnetic susceptibility, it was concluded[160] that the growth of $\chi(T)$ is not due to local magnetic moments. This effect is most likely due to spin fluctuations in the vanadium vacancy layers. An unusually strong effect of magnetic field on T_N was also noted:

$$\frac{T_N(H)}{T_N(0)} \sim 1 - \left(\frac{H}{H_c}\right)^4,$$

where $H_c = 75.6$ kOe.

Analysis of the experimental situation leaves no doubt as to the itinerant nature of the antiferromagnetism of V_3X_4 and V_5X_8. Band-structure calculations have not been done for any of these materials, but results of a calculation for the isoelectronic and isostructural niobium compounds Nb_3X_4 have recently been published.[161] The Fermi surface of these substances consists of a system of rippled (to varying degrees) sheets parallel to the basal plane of the hexagonal Brillouin zone. One pair of these sheets is separated by a vector $\mathbf{G}_2$, so that in the antiferromagnetic phase there should be a doubling of the period along the hexagonal axis. It was just such a magnetic structure that was assumed in the experimental papers discussed above.

Thus there is every reason to assume that the antiferromagnetism of V_3X_4 can be described in the excitonic insulator model. In the case of V_5X_8 the situation is more complicated, since in this case there are three nonequivalent layers of vanadium atoms (a completely filled layer and two types of vacancy layers), whereas in V_3X_4 there is only one type of vacancy layer. The band structure of V_5X_8 is unknown. Nevertheless, it can be assumed that the antiferromagnetism here is of the same nature as in V_3X_4.

Magnetic-susceptibility and neutron-diffraction measurements of the hexagonal modification of *nickel monosulfide* (NiS) have revealed a transition to an antiferromagnetic phase below $T_N = 265$ K.[162] This transition is accompanied by a jump in the resistance by almost two orders of magnitude, by thermal hysteresis, and by a specific-heat anomaly,[162] i.e., the transition to the antiferromagnetic phase is simultaneously a metal-insulator transition. A detailed discussion of the metal-insulator transition in NiS is given in Ref. 163.

At the present time there is no consistent theoretical interpretation of the properties of NiS, but several circumstances permit the assumption that the antiferromagnetism in this material is due to a spin-density wave. First of all, above T_N it has been found[162] that there is no magnetic diffractive scattering of neutrons, and the temperature dependence of the magnetic susceptibility is typical for ordinary

Pauli itinerant paramagnets. Furthermore, below T_N a magnetic moment of $1\mu_B$ per Ni atom arises discontinuously and grows to $1.66\mu_B$ at $T = 4.2$ K. Finally, the band-structure calculations of Ref. 164 have shown that the paramagnetic phase has nearly nested portions of the electron and hole Fermi surface (the Γ–M direction).

It is interesting to note that the nesting wave vector $\tilde{\mathbf{Q}}$ for these portions is equal to zero. According to the band calculation,[164] in the antiferromagnetic phase the nested portions (and all the other parts of the Fermi surface that exist in the paramagnetic phase) vanish completely, and an insulator gap arises. If it is assumed that these are the parts responsible for the formation of the SDW, then we encounter a situation in which a one-dimensional triplet order parameter appears. Kozlov and Maksimov[17] discuss just such a situation; it corresponds to itinerant antiferromagnetism without a period doubling. The average moment of the unit cell is equal to zero, but within the cell there is an antiferromagnetic redistribution of the spin density.

The main obstacle to the direct application of the excitonic insulator model to NiS is the strong first-order character of the transition. This property may be due to a strong spin polarization of the electron reservoir, i.e., of the nonsingular parts of the Fermi surface, in the field of the SDW or to the spin-lattice interaction. Howeve, there have been no detailed calculations for NiS (only a qualitative discussion[164] of the two-band excitonic insulator model). On the other hand, the large value of the local moment per Ni atom indicates that single-site electron correlations play an important role. For this reason it may be necessary to incorporate spin-fluctuation effects, in the spirit of local-spin-fluctuation theory.

An extremely interesting object of study is the *helical magnet* MnSi, for which $T_N = 20$ K (Ref. 165) and the magnetic moment in the ordered state is $0.4\mu_B$ at $T = 4.2$ K. The wave vector of the helical structure is directed along the (111) axis of the cubic lattice, and the wavelength is extraordinarily large: 180 Å.

According to measurements of the NMR, resistance, and entropy change at the transition point, MnSi is classified as a weak intinerant magnet. However, the temperature dependence of the susceptibility[166] obeys the Curie-Weiss law above T_N all the way up to 300 K, after which it increases with temperature. Recent inelastic-neutron-scattering measurements have revealed the presence of strong spin fluctuations both above and below T_N, while in an earlier paper by the same authors[168] it was found that the magnetic moment per Mn atom increases(!) with increasing temperature in the paramagnetic phase. This situation may be due, on the one hand, to a disorientation of the moments at the Mn atoms and, on the other, to a change in the spin density of the d-electrons with temperature. The nature of this change could be different (see, e.g., the mechanism proposed by Edwards[172]).

The cause of the helical magnetism in MnSi, whose lattice lacks a center of inversion, has been linked in a purely qualitative way[169] to relativistically small interactions which give rise to invariants of the Dzyaloshinskiĭ-Moriya type in the expansion of the free energy.

The available band-structure calculation[170] for MnSi indicates that there are no nested portions of the Fermi surface at the wave vector of the helical structure. At first glance this would seem to be an important argument against the use of the excitonic insulator model. However, because of the small size of the wave vector of the magnetic structure one can propose an original mechanism for the onset of the helical ordering.[171] This mechanism, which is related to the "excitonic-ferromagnetism" model proposed by Volkov and Kopaev,[18] can be represented (as it applies to MnSi) in the following way.

In the hypothetical high-temperature protophase of MnSi, which has the NaCl structure, the Fermi surface has nested portions which cause a structural instability. The actual crystal structure of MnSi is obtained from the NaCl protophase by displacing the Mn and Si atoms in such a way that the fcc unit cell with two atoms in the basis is transformed into a simple cubic cell with eight atoms. With respect to the protophase such a structural transition can be treated as the onset of a CDW. If against the background of the CDW there now arises a helical SDW with a period slightly different from that of the CDW, then with respect to the actual MnSi structure this will look like the onset of a long-period magnetic structure with a wave vector determined by the difference between the wave vectors of the CDW and SDW. In the observed crystal structure of MnSi the nested portions of the protophase are covered by the gap and, naturally, cannot determine the topology of the Fermi surface. It is pertinent to note that it was a study of the genesis of the actual crystal structure of IV–VI semiconductors from a protophase with nested portions that enabled Volkov and Pankratov[177] to explain the structural phase transitions in these systems.[177]

There is a large class of magnets for which it has been established that the magnetic ordering is due to both the SDW-instability mechanism and the presence of local magnetic moments. For example, in the case of alloys of Cr and Y with heavy rare earth metals the local magnetic moments are due to the f electrons of the inner shell of the rare earth ion. In the case of transition metals the "localization" of the magnetic moment is due to the spatial dependence of the spin density of the band electrons, $m(\mathbf{r}) = \rho\uparrow(\mathbf{r}) - \rho\downarrow(\mathbf{r})$. Strictly speaking, here one cannot divide the electrons into band electrons and localized electrons, and it is necessary to construct a theoretical model combining the properties of the excitonic insulator model, which incorporates the topological features of the Fermi surface, and the properties of some spin-fluctuation model. In addition to the previously discussed alloys of Cr with Fe and Co, substances of this type include, in particular, alloys of iron with rhodium (FeRh) and platinum (Pt_3Fe)[174,175] and an alloy of nickel and manganese (NiMn].[176]

Magnel Phases, V_nO_{2n+1}. Kopaev and coauthors[178,179] have proposed a mechanism for the structural and antiferromagnetic transitions in these compounds on the basis of the excitonic insulator model. The excitonic insulator model applies in this case because the Fermi surface of the compound VO_2 has nested portions separated by a wave vector $\tilde{\mathbf{Q}} = (1/$

2, 0, 1/2) along the ΓR direction.[180] The idea has been expressed[178] that Magnel phases with $n \neq \infty$ have a narrow band formed by oxygen vacancies. This band lies below the Fermi level, and therefore the excess electrons supplied by the oxygen vacancies do not change the position of the Fermi level, and the band remains nested.

The experimental situation in Magnel phases is as follows: in VO_2 there is a metal-insulator transition with a change in the crystal symmetry at $T_c = 340$ K; in the series $V_n O_{2n+1}$ $(2 < n < 9)$ at temperatures $T_N < T_c$ there is an antiferromagnetic transition; in V_2O_3 the Néel temperature T_N equals T_c, and the antiferromagnetic transition occurs with a change in the crystal symmetry.

A phenomenological model giving a qualitative explanation of these features of the Magnel phases was considered in Ref. 179. This model is based on a two-parameter Landau expansion for the free energy (the singlet and triplet order parameters which, in the excitonic insulator model, are responsible for the structural and antiferromagnetic transitions, respectively). An important role is played by the Coulomb interaction of the CDW with vacancies (which, according to Ref. 178, form chains along the C_2 axis) and by the Coulomb interaction of charges on neighboring chains. The latter gives rise to an ordering of vacancies both along the chains and in the transverse direction (it is advantageous to have a positive charge on one chain located across from the center of negative charge on the neighboring chain). The qualitative phase diagram of Ref. 179 is reproduced in Fig. 18. The solid line $T_c(1/n)$ is the theoretical line of the first order transition to the insulating phase, while the solid line $T_N(1/n)$ is the theoretical line of the second order transition to the antiferromagnetic phase. The dashed line shows the experimental curve of $T_c(1/n)$. The sharp drop in $Tc(1/n)$ observed in experiment [around $n = 6$–8 we have $T_c < T_N$, and for $n = 7$ we have $T_c(1/7) = 0$] was attributed in Ref. 179 to the strong scattering of the CDW by incompletely ordered oxygen vacancies (at large values $1/n > 1/4$ the vacancies are ordered, while at small values of $1/n$ the vacancy concentration is small and vacancy scattering is unimportant).

8. CONCLUSION

In summing up this review, we can say that the active theoretical and experimental research in recent years has yielded substantial progress in our understanding of the nature of the antiferromagnetism of chromium and its dilute alloys. However, several unresolved questions remain.

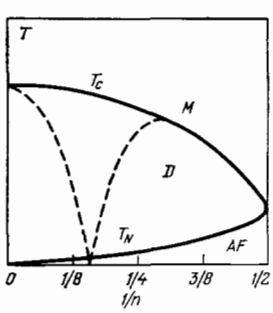

FIG. 18. Phase diagram for the phases of Magnel $V_n O_{2n-1}$.[179]

1. Collective excitations in the incommensurate SDW structure. It was recently reported[63] that a new low-frequency mode of excitations has been observed in highly pure Cr samples. These excitations can be interpreted as oscillations of domain walls (oscillations of the SDW soliton lattice). No theoretical calculation of the spectrum of excitations of this type has been done for Cr.

2. The role of the lattice in the formation of an incommensurate SDW and in the transition between the I and C phases. Experiment shows that the I-C transition in Cr alloys has a much more pronounced first-order character than is implied by model calculations[113] which ignore the electron-phonon interaction, and the corresponding experimental line $T_{IC}(\mu)$ agrees poorly with experiment.

3. Anomalies (mentioned previously) in alloys of chromium with nontransition elements and magnetic $3d$ metals. In the first case it is necessary to introduce an internal structure of the impurity (in particular, possible resonance levels). In the second case we are evidently up against the complex problem of the formation of a local magnetic moment in the presence of a peculiar topology of the Fermi surface.

In other systems with a SDW instability there has been no substantial progress. The reason for this is, on the one hand, that there has been insufficient experimental interest in these systems and, on the other, that even the existing data have not been subjected to a consistent theoretical interpretation. In this situation the excitonic insulator model should be regarded as more of a fundamental conceptual basis than a method for quantitative calculation. Actual systems require many complications and modifications of the theory, and the existing results obtained in the excitonic insulator model for systems with a SDW instability cannot be transferred mechanically to these new systems. We hope that the present review will in some measure stimulate greater research activity in these interesting systems.

We wish to thank L. V. Keldysh for interest in this article and for a number of valuable comments made during a discussion of it. We are also indebted to Yu. V. Kopaev and D. I. Khomskiĭ for many helpful comments and friendly criticism, and to B. A. Volkov and B. G. Idlis for discussion of individual questions.

[1]J. C. Slater, *The Self-Consistent Field for Molecules and Solids*, McGraw-Hill, New York (1963). [Russ. Transl. Mir, M., 1978).
[2]T. M. Rice, A. S. Barker, Jr., B. I. Halperin, and D. B. McWhan, J. Appl. Phys. **40**, 1337 (1969).
[3]L. Corliss, J. Hastings, and R. Weiss, Phys. Rev. Lett. **3**, 211 (1959); V. N. Bykov, V. S. Golovkin, N. V. Ageev, V. A. Levdik, and S. I. Vinogradov, Dokl. Akad. Nauk SSSR **128**, 1153 (1959) [Sov. Phys. Dokl. **4**, 1070 (1960)].
[4]S. A. Werner, A. Arrot, and H. Kendrick, Phys. Rev. **155**, 528 (1967); E. Fawcett, R. Griessen, and C. Vettier, Proceedings of International Conference on Transition Metals, Toronto, Inst. Phys. Conf. Ser., No. 39 (1978), p. 592.
[5]A. Arrot, S. A. Werner, and H. Kendrick, Phys. Rev. Lett. **14**, 1022 (1965).
[6]G. Shirane and W. Takei, J. Phys. Soc. Jpn. **17**, Suppl. B-III, 35 (1962).
[7]S. N. Behera and K. S. Viswanathan, Can. J. Phys. **47**, 477 (1969).
[8]A. K. Butylenko and N. S. Kobzenko, in: *Metallofizika*, No. 65, Naukova Dumka, Kiev (1976), p. 60.
[9]T. Moriya, in: *Electron Correlation and Magnetism in Narrowband Systems*, (ed. by T. Moriya), Springer-Verlag, New York (1981).

[10]A. W. Overhauser, Phys. Rev. **128**, 1437 (1962).
[11]A. K. Rajagopal, Phys. Rev. **142**, 152 (1966); D. R. Hamann and A. W. Overhauser, Phys. Rev. **143**, 183 (1966).
[12]W. M. Lomer, Proc. Phys. Soc. London **80**, 489 (1962).
[13]P. A. Fedders and P. C. Martin, Phys. Rev. **143**, 245 (1966).
[14]L. V. Keldysh and Yu. V. Kopaev, Fiz. Tverd. Tela (Leningrad) **6**, 2791 (1964) [Sov. Phys. Solid State **6**, 2219 (1965)].
[15]B. I. Halperin and T. M. Rice, Solid State Phys. **21**, 125 (1968).
[16]J. De Cloizeaux, J. Phys. Chem. Solids **26**, 259 (1965).
[17]A. N. Kozlov and L. A. Maksimov, Zh. Eksp. Teor. Fiz. **48**, 1184 (1965) [Sov. Phys. JETP **21**, 790 (1965)].
[18]B. A. Volkov and Yu. V. Kopaev, Pis'ma Zh. Eksp. Teor. Fiz. **27**, 10 (1978) [JETP Lett. **27**, 7 (1978)].
[19]Yu. V. Kopaev, Tr. FIAN **86**, 3 (1975).
[20]K. W. Buker, Phys. Rev. B **24**, 5713 (1981).
[21]A. A. Abrikosov, L. P. Gor'kov, and I. E. Dzyaloshinskiĭ, *Metody kvantovoĭ teorii polya v statistecheskoĭ mekhanike*, Fizmatgiz, Moscow (1962) [*Methods of Quantum Field Theory in Statistical Physics*, Prentice-Hall, Englewood Cliffs, N. J. (1963)].
[22]T. M. Rice, Phys. Rev. B **2**, 3619 (1970).
[23]Yu. V. Kopaev, Fiz. Tverd. Tela (Leningrad) **12**, 3 (1970) [Sov. Phys. Solid State **12**, 1 (1970)].
[24]J. Zittartz, Phys. Rev. **164**, 575 (1967); H. Everts and J. Zittartz, J. Low Temp. Phys. **11**, 1306 (1973).
[25]Yu. V. Kopaev and A. I. Rusinov, Fiz. Tverd. Tela (Leningrad) **11**, 1306 (1969) [Sov. Phys. Solid State **11**, 1059 (1969)]; Yu. V. Kopaev and R. Kh. Timerov, Fiz. Tverd. Tela (Leningrad) **13**, 122 (1971) [Sov. Phys. Solid State **13**, 96 (1971)]; Do Chan Kat, Yu. V. Kopaev, and R. Kh. Timerov, Fiz. Tverd. Tela (Leningrad) **15**, 537 (1973) [Sov. Phys. Solid State **15**, 372 (1973)].
[26]E. Fenton and C. Leavens, J. Phys. F **10**, 1853 (1980).
[27]S. V. Vonsovskiĭ, Yu. A. Izyumov, and É. Z. Kurmaev, *Sverkhprovodimost' perekhodnykh metallov, ikh splavov i soedineniĭ* [Superconductivity of Transition Metals and of Their Alloys and Compounds], Nauka, Moscow (1977).
[28]N. I. Kulikov and V. V. Tugushev, J. Phys. C **14**, L809 (1981).
[29]J. R. Kelly, C. A. Moyer, and S. Arajs, Phys. Rev. B **20**, 1099 (1979).
[30]B. Lebech and K. Mikke, J. Phys. Chem. Solids **63**, 1651 (1972).
[31]A. K. Butylenko and V. V. Nevdacha, Dokl. Akad. Nauk Ukr. SSR Ser. A **5**, 67 (1980).
[32]W. C. Koehler, R. M. Moon, A. L. Trego, and A. R. Mackintosh, Phys. Rev. **151**, 405 (1966).
[33]B. M. Geerken, R. Griessen, G. Benediktsson, H. U. Astrom, and C. van Dijk, J. Phys. F **12**, 1603 (1982).
[34]T. J. Bastow, Proc. Phys. Soc. London A **88**, 935 (1966).
[35]Y. Hamagushi, E. O. Wollan, and W. C. Koehler, Phys. Rev. **138**, A737 (1965).
[36]T. I. Kostina, V. Yu. Galkin, E. I. Kondorskiĭ, and A. B. Katyrenchuk, Fiz. Met. Metalloved. **40**, 851 (1975).
[37]L. G. Maĭstrenko and B. M. Polovov, Fiz. Met. Metalloved. **43**, 991 (1977).
[38]A. K. Butylenko and V. V. Nevdacha, Ukr. Fiz. Zh. **26**, 1390 (1982).
[39]S. Iida, M. Kohno, Y. Tsunoda, and N. Kutitomi, J. Phys. Soc. Jpn. **44**, 1747 (1978).
[40]E. Fawcett and C. Vettier, J. Phys. (Paris) **43**, 1365 (1982).
[41]W. L. McMillan, Phys. Rev. B **14**, 1496 (1978).
[42]P. Back and J. Timonen, J. Phys. C **11**, 4901 (1978).
[43]D. F. Litvin and E. G. Ponyatovskiĭ, Dokl. Akad. Nauk SSSR **156**, 69 (1964) [Sov. Phys. Dokl. **9**, 388 (1964)].
[44]F. F. Voronov, Zh. Eksp. Teor. Fiz. **47**, 1999 (1964) [Sov. Phys. JETP **20**, 1342 (1965)].
[45]T. Mitsui and C. T. Tomisuka, Phys. Rev. **137**, A564 (1965).
[46]A. Jayraman, T. M. Rice, and E. Bucher, J. Appl. Phys. **41**, 869 (1970).
[47]A. K. Butylenko and V. V. Nevdacha, Ukr. Fiz. Zh. **25**, 137 (1980).
[48]N. Mori, Y. Fukada, and T. Mitsui, J. Phys. Soc. Jpn. **28**, 531 (1970).
[49]W. De Dood, J. de Dood, and P. F. Chatel, Physica (Utrecht) **47**, 846, 337 (1970).
[50]D. B. McWhan and T. M. Rice, Phys. Rev. Lett. **19**, 846 (1967).
[51]T. Moriya, J. Magn. Magn. Mater. **14**, 1 (1979).
[52]H. Hasegawa, J. Phys. Soc. Jpn. **49**, 178 (1980).
[53]I. Pop and D. Dabarlet *et al.*, J. Phys. Chem. Solids **92**, 927 (1981).
[54]J. Sousa *et al.*, J. Phys. (Paris) **39**, C-6, 792 (1978); J. Phys. F. **10**, 2535 (1980).
[55]H. Alberts and S. Burger, Solid State Commun. **28**, 771 (1978).
[56]V. I. Grebennikov, Yu. I. Prokop'ev, O. B. Sokolov, and E. A. Turov, Fiz. Met. Metalloved. **54**, 896 (1982).
[57]K. Fukamichi, J. Phys. F **9**, L85 (1979).
[58]G. Benediktsson, L. Hedman, H. Astrom, and K. Rao, J. Phys. F **12**, 1439 (1982).
[59]S. N. Evangelou, H. Hasegawa, and D. M. Edwards, J. Phys. F **12**, 2035 (1982).
[60]A. Jayaraman, R. Maines, K. Rao, and S. Arajs, Phys. Rev. Lett. **37**, 926 (1976).
[61]S. Arajs *et al.*, Phys. Lett. A **45**, 175 (1972).
[62]S. Arajs *et al.*, Nuovo Cimento **48**, 40 (1971).
[63]G. R. Fincher, G. Shirane, and S. A. Werner, Phys. Rev. B **24**, 1312 (1981).
[64]T. Suzuki, J. Phys. Soc. Jpn. **43**, 869 (1977).
[65]J. Takashi *et al.*, J. Phys. Soc. Jpn. **49**, 1480 (1980).
[66]Y. Endoch, J. Mizuki, and Y. Ishikawa, J. Phys. Soc. Jpn. **51**, 2828 (1982).
[67]J. Mizuki, Y. Endoch, and Y. Ishikawa, J. Phys. Soc. Jpn. **51**, 3497 (1982).
[68]T. Suzuki, J. Phys. Soc. Jpn. **45**, 1852 (1978).
[69]S. Arajs, R. Aidun, and C. Moyer, Phys. Rev. B **22**, 5366 (1980).
[70]S. Iida, S. Kawarazaki, and K. Kunitomi, J. Phys. Soc. Jpn. **50**, 3612 (1981).
[71]J. Mizuki and Y. Endoch, J. Phys. Soc. Jpn. **51**, 3508 (1982).
[72]K. Fukamishi, Phys. Status Solidi A **49**, K37 (1978).
[73]T. Sano, S. Kawarazaki, S. Iida, and N. Kanitomi, J. Phys. Soc. Jpn. **50**, 1203 (1981).
[74]S. Asano and J. Yamashita, J. Phys. Soc. Jpn. **23**, 714 (1967).
[75]J. Rath and J. Callaway, Phys. Rev. B **8**, 5398 (1973).
[76]N. I. Kulikov, Fiz. Nizk. Temp. **5**, 173 (1979) [Sic].
[77]D. G. Laurent, J. Callaway, J. L. Fry, and N. E. Brener, Phys. Rev. B **23**, 4977 (1981).
[78]J. E. Graebner and J. Marcus, Phys. Rev. **175**, 659 (1968).
[79]E. Fawcett, R. Griessen, and D. J. Stanley, J. Low Temp. Phys. **25**, 771 (1976).
[80]L. I. Vinokurova, A. G. Gapotchenko, E. S. Itskevich, É. T. Kulatov, and N. I. Kulikov, Pis'ma Zh. Eksp. Teor. Fiz. **30**, 265 (1979) [JETP Lett. **30**, 246 (1979)].
[81]R. Reifenberger, F. W. Holroyd, and E. Fawcett, J. Low Temp. Phys. **38**, 421 (1980).
[82]W. J. Venema, R. Griessen, and W. F. Ruesink, J. Phys. F **10**, 2841 (1980).
[83]L. M. Falikov and M. J. Zuckermann, Phys. Rev. **160**, 372 (1967).
[84]A. J. Arko, J. A. Marcus, and W. A. Reed, Phys. Rev. **176**, 671 (1968); **185**, 901 (1969).
[85]E. Fawcett, F. W. Holroyd, and R. Reifenberger, J. Low Temp. Phys. **38**, 421 (1980).
[86]H. Umebayshi, G. Shirane, B. C. Frazer, an W. H. Daniels, J. Phys. Soc. Jpn. **24**, 318 (1968).
[87]E. J. Gutman and J. L. Stendford, Phys. Rev. B **4**, 4020 (1971).
[88]S. Komura, Y. Hamagushi, and N. Kunitomi, J. Phys. Soc. Jpn. **23**, 171 (1967).
[89]D. W. Ruesink, J. M. Pertz, and I. M. Templeton, Phys. Rev. Lett. **45**, 734 (1980).
[90]N. I. Kulikov and . T. Kulatov, J. Phys. F **12**, 2291 (1982).
[91]J. Kübler, J. Magn. Magn. Mater. **20**, 277 (1980).
[92]H. L. M. Bakker, R. Griessen, and W. F. Venema, J. Phys. F **10**, 833 (1980).
[93]J. F. Shirber, Phys. Lett. A **35**, 194 (1971).
[94]E. W. Fenton, Solid State Commun. **32**, 195 (1979).
[95]K. Nakanishi and K. Maki, Prog. Theor. Phys. **48**, 1059 (1972).
[96]A. I. Larkin and Yu. N. Ovchinnikov, Zh. Eksp. Teor. Fiz. **47**, 1136 (1964) [Sov Phys. JETP **20**, 762 (1965)].
[97]P. Fulde and R. A. Ferell, Phys. Rev. **135**, A550 (1964).
[98]A. Malaspinas and T. M. Rice, Phys. Kondens. Mater. **13**, 193 (1971).
[99]A. Shibatani, K. Motizuki, and T. Nagamiya, Phys. Rev. **17**, 984 (1969).
[100]A. Shibatani, J. Phys. Soc. Jpn. **29**, 93 (1970).
[101]A. Kotani, J. Phys. Soc. Jpn. **38**, 974 (1975).
[102]K. Nakanishi and T. Kasuya, J. Phys. Soc. Jpn. **42**, 833 (1977).
[103]B. A. Volkov and V. V. Tugushev, Zh. Eksp. Teor. Fiz. **77**, 2104 (1979) [Sov. Phys. JETP **50**, 1006 (1979)].
[104]Vl. A. Gurevich and B. A. Volkov, Fiz. Nizk. Temp. **5**, 1419 (1979) [Sov. J. Low Temp. Phys. **5**, 670 (1979)].
[105]Y. Tsunoda, M. Mori, N. Kunitomi, Y. Teraoka, and J. Kanamori, Solid State Commun. **14**, 287 (1974).
[106]C. F. Eagen and S. A. Werner, Solid State Commun. **16**, 1113 (1975).
[107]R. Pynn, W. Press, S. M. Shapiro, and S. A. Werner, Phys. Rev. B **13**, 295 (1976).
[108]S. Iida, M. Kohno, Y. Tsunoda, and N. Kunitomi, J. Phys. Soc. Jpn. **44**, 1747 (1978).

[109]S. Iida, M. Kohno, Y. Tsunoda, and N. Kunitomi, J. Phys. Soc. Jpn. **50**, 2581, 2587 (1981).
[110]Y. Tsunoda, Y. Nakei, and N. Kunitomi, Solid State Commun. **16**, 443 (1975).
[111]S. Nakajima and Y. Kurihara, J. Phys. Soc. Jpn. **38**, 330 (1975).
[112]A. Kotani, J. Phys. Soc. Jpn. **39**, 851 (1975); **41**, 1473 (1976); **44**, 1455 (1978); **45**, 766 (1978).
[113]A. I. Buzdin and V. V. Tugushev, Fiz. Tverd. Tela (Leningrad) **25**, 882 (1983) [Sov. Phys. Solid State **25**, 506 (1983)]; Zh. Eksp. Teor. Fiz. **85**, 735 (1983) [Sov. Phys. JETP **58**, 428 (1983)].
[114]S. A. Brazovskiĭ, S. A. Gordyunin, and N. N. Kirova, Pis'ma Zh. Eksp. Teor. Fiz. **31**, 486 (1980) [JETP Lett. **31**, 456 (1980)].
[115]B. Horovitz, Phys. Rev. Lett. **48**, 1416 (1982).
[116]A. Kotani and I. Harada, J. Phys. Soc. Jpn. **51**, 1737 (1982).
[117]Y. Nakai and S. Iida, J. Phys. Soc. Jpn. **50**, 3637 (1981).
[118]L. W. Bos and D. W. Lynch, Phys. Rev. B **2**, 4567 (1970).
[119]M. B. Walker, Phys. Rev. Lett. **44**, 1261 (1980); Phys. Rev. B **22**, 1338 (1981).
[120]Z. Barak and M. B. Walker, J. Phys. F **12**, 483 (1982).
[121]E. W. Fenton, Phys. Rev. Lett. **45**, 736 (1980); J. Phys. C **14**, 4217 (1981).
[122]H. J. Brocksch, H. U. Everts, and H. Muller-Krumbhaar, J. Phys. C. **14**, 603 (1981).
[123]A. Shibatani, J. Phys. Soc. Jpn. **31**, 1642 (1971).
[124]K. Maki and M. Sakurai, Prog. Theor. Phys. **47**, 1110 (1972).
[125]H. L. Skriver, J. Phys. F **11**, 97 (1981).
[126]S. H. Liu, Phys. Rev. B **2**, 2664 (1970).
[127]C. A. Moyer, S. Arajs, and L. Hedman, Phys. Rev. B **14**, 1233 (1976).
[128]S. Ami and W. Young, J. Phys. F **11**, 227 (1981).
[129]K. H. Oh, B. N. Harmon, S. H. Liu, and S. K. Sinha, Phys. Rev. B **14**, 1283 (1976).
[130]M. Yasui and M. Shimizu, J. Phys. F **9**, 1653 (1979).
[131]R. P. Gupta and S. K. Sinha, Phys. Rev. B **3**, 2401 (1971).
[132]J. B. Sokoloff, Phys. Rev. **185**, 770 (1969).
[133]S. K. Sinha, S. H. Liu, L. D. Mahlestein, and N. Wakabayashi, Phys. Rev. Lett. **23**, 311 (1969).
[134]J. Als-Wielsen, J. D. Axe, and G. Shirane, J. Appl. Phys. **42**, 1668 (1971).
[135]S. Ami and W. Young, J. Phys. F **11**, 1913 (1981).
[136]B. Fisher, J. Phys. F **2**, 806 (1972).
[137]S. H. Liu, J. Magn. Magn. Mater. **25**, 97 (1981).
[138]K. Ziebeck, J. Booth, P. Brown, J. Capellman, and J. Bland, Z. Phys. **848**, 233 (1982).
[139]B. T. Matthias, A. L. Giorgi, V. D. Struebing, and J. L. Smith, J. Phys. (Paris) Lett. **39**, L441 (1978); Phys. Lett. A **69**, 221 (1978).
[140]F. Asker, Z. Fisk, J. L. Smith, and C. Y. Huang, J. Magn. Magn. Mater. **22**, 250 (1981).
[141]P. Manod, I. Felner, G. Chouteau, and D. Shaltiel, J. Phys. (Paris) Lett. **41**, L511 (1980); D. Shaltiel, P. Monod, and I. Felner, J. Phys. (Paris) **41**, 587 (1980).
[142]G. R. Stewart, B. T. Matthias, A. L. Giorgi, E. G. Szklarz, and J. L. Smith, Solid State Commun. **30**, 709 (1979); C. P. Enz and G. R. Stewart, Solid State Commun. **35**, 951 (1980).
[143]C. P. Enz. Phys. Rev. B **25**, 6822 (1982).
[144]R. A. De Groot, D. D. Koelling, and F. M. Mueller, J. Phys. F **10**, L235 (1980).
[145]T. Jarlborg and A. J. Freeman, Phys. Rev. B **22**, 2332 (1980).
[146]A. L. Giorgi, B. T. Matthias, G. R. Stewart, J. Asker, and J. L. Smith, Solid State Commun. **32**, 455 (1979).
[147]A. L. Giorgi and G. R. Stewart, Solid State Commun. **44**, 1465 (1982).
[148]R. L. Barnes and P. G. Crel, Phys. Lett. A **29**, 203 (1969).
[149]J. Castaing, P. Costa, M. Haritier, and P. Lederer, J. Phys. Chem. Solids **33**, 533 (1972).
[150]J. Castaing, J. Danan, and M. Rieux, Solid State Commun. **10**, 563 (1972).
[151]S. H. Liu, L. Kopp, W. B. England, and H. W. Myron, Phys. Rev. B **11**, 3463 (1975).
[152]I. Kawada *et al.*, J. Solid State Chem. **15**, 246 (1975).
[153]G. V. Samsonov and I. M. Vinitskiĭ, *Tugoplavkie Soedineniya* [Refractory Compounds], Metallurgiya, Moscow (1976).
[154]I. Tsubokawa, J. Phys. Soc. Jpn. **14**, 196 (1959).
[155]W. S. England, S. H. Liu, and H. W. Myron, J. Chem. Phys. **80**, 3760 (1974).
[156]S. H. Liu, Phys. Rev. B **10**, 3619 (1974).
[157]Y. Kitaoka, H. Yasuoka, Y. Oka, and K. Kosuya, J. Phys. Soc. Jpn. **46**, 1381 (1979).
[158]Y. Tuzuka, T. Sato, and Y. Miyako, J. Phys. Soc. Jpn. **51**, 2131 (1982).
[159]N. Nishihara, H. Yasuoka, Y. Oka, K. Kosuya, and S. Kachi, J. Phys. Soc. Jpn. **42**, 787 (1977).
[160]Y. Kitaoka, H. Yasouka, J. Phys. Soc. Jpn. **48**, 1460 (1980).
[161]A. Oshiyama, J. Phys. Soc. Jpn. **52**, 587 (1983); Solid State Commun. **43**, 607 (1982).
[162]J. T. Sparks and T. Komoto, Rev. Mod. Phys. **40**, 752 (1968).
[163]G. V. Loseva and S. O. Ovchinnikov, in: *Fizika magnitnykh materialov* [Physics of Magnetic Materials], Nauka, Novosibirsk (1983).
[164]L. F. Mattheiss, Phys. Rev. B **10**, 995 (1974).
[165]I. Ishikawa, K. Tajima, D. Bloch, and M. Roth, Solid State Commun. **19**, 525 (1976).
[166]H. Yasuoka, J. Phys. Soc. Jpn. **44**, 842 (1978).
[167]K. Ziebeck, H. Capellmann, P. Brown, and J. Booth, Z. Phys. B **48**, 241 (1982).
[168]K. Ziebeck and P. Brown, J. Phys. F **10**, 2015 (1980).
[169]O. Nakanishi, A. Yanase, and A. Hasegawa, Solid State Commun. **35**, 995 (1980).
[10]D. Nakamishi, A. Yanase, and M. Kataoka, in: *Electron Correlation and Magnetism in Narrowband Systems*, (ed. by T. Moriya,) Springer-Verlag, New York (1981), p. 126.
[171]B. A. Vokov and V. V. Tugushev, Zh. Eksp. Teor. Fiz. **77**, 2104 (1979) [Sov. Phys. JETP **50**, 1006 (1979)].
[172]D. Edwards, J. Phys. F **12**, 1789 (1982).
[173]R. B. Roberts, G. K. White, and E. Fawcett, Physica B **119**, 63 (1983).
[174]N. I. Kulikov, E. T. Kulatov, L. I. Vinokurova, and M. Pardavi-Horvath, J. Phys. F **12**, L91 (1982).
[175]N. I. Kulikov, E. T. Kulatov, and S. I. Yakhimovich, J. Phys. F **14**, (1984); N. I. Kulikov, J. Phys. F **14** (1984).
[176]V. E. Egorushkin, S. N. Kul'kov, and S. E. Kul'kova, Zh. Eksp. Teor. Fiz. **84**, 599 (1983) [Sov. Phys. JETP **57**, 345 (1983)].
[177]B. A. Volkov and S. A. Pankratov, Zh. Eksp. Teor. Fiz. **75**, 1362 (1978) [Sov. Phys. JETP **48**, 687 (1978)].
[178]Yu. V. Kopaev and V. G. Mokerov, Dokl. Akad. Nauk SSSR **264**, 1370 (1982) [Sov. Phys. Dokl. **27**, 487 (1982)].
[179]B. G. Idlis and Yu. V. Kopaev, Solid State Commun. **45**, 301 (1983).
[180]M. Gupta, A. Freeman and D. Ellis, Phys. Rev. B **16**, 3338 (1977).

Translated by Steve Torstveit